Authors’ response to RC1 and RC2

Manuscript number: acp-2019-555

The Vertical Variability of Black Carbon Observed in the Atmospheric Boundary Layer during DACCIWA by Barbara Altstädter et al.

First, the authors acknowledge both referees for sharing their valuable comments! The authors agree that the goal of the study was not exactly formulated in the previous manuscript. Please, take into account the changes in the marked-up manuscript. The sections “Abstract” and “Conclusion” were completely revised. Further, the new manuscript will benefit from a more detailed description of the technical part. For instance, the explanation of “phase shift free low pass filtering” and information on data treatment were extended. We agree that this is mandatory in order to sufficiently describe the used methods for a broader range of ACP readers.

Before starting the responses, just some short hints in advance:

The authors will take into account the editorial support for the revised manuscript. Language issues were criticised by both referees and might have led to misunderstandings in the discussion paper.

Please note that some literature was updated during review process. The current references are listed at the end of the authors’ response and were added to the marked-up manuscript.

Now, find attached the authors’ response according to the two referee comments (RC1 and RC2) in a point-by-point way. The changes are marked in the annotated manuscript enclosed to this response.

Comments of referee #1 (RC1)

“This paper describes aethalometer measurements made using a UAV in West Africa. While the measurement capability is interesting, I have some fundamental concerns with the appropriateness of the aethalometer as a measurement tool and the described data treatment. Also, the paper needs to be sharpened considerably to highlight the main messages and to put them in context so that readers can easily see the value of the findings; in my opinion it will require a major revision to be publishable in ACP. Below I include, first, my major comments and then smaller issues/recommended edits.”

Author’s response to referee #1

The authors thank the anonymous referee for the critical and thorough reading and for providing specific comments that will improve the current manuscript. We agree that data post-processing should be described more in detail in order to make it clear for all disciplines of ACP.

Point-to-point response:

RC1: *“1. The microaethelometer is not a very robust tool to measure BC. I believe that this paper serves as the first detailed description and evaluation of the AE51 on ALADINA (the cited reference by Bärfuss shows a profile but says that the measurement is, as yet, unverified). There are some published studies evaluating its performance but, to my knowledge, not on airborne platforms, and often not in comparison to a verifiable BC measurement.”*

Authors’ response:

The authors agree that the micro aethalometer is not the most reliable tool for detecting BC. However, it is very feasible for UAS operation, as integration of new sensors is mostly restricted by limitations of weight and size. The size of AE51 is small and the weight is not exceeding more than 300 g!

It was used for some studies on light airborne platforms like UAS and tethered balloons (e.g. Chilinski et al., 2018; Ferrero et al., 2014). To our current knowledge, the AE51 was not tested on manned aircraft simultaneously with so called “reliable tools” (e.g. MAAP, SP2) so far. If we missed out any literature, we would be grateful for further information.

Before answering in full, the authors want to take the opportunity to explain the missing comparison of airborne BC data with other BC methods/stations/institutes that would be definitely helpful to verify the shown data. This is not foreseen as any excuse, but it would help to understand the chosen validations and the results why comparing AE51 data with filter samples and COSMO-ART model, as it is shown in the manuscript. Please note that the micro aethalometer was implemented on the UAS ALADINA during DACCIWA, but it was not the main goal to study BC during the aircraft field campaign. The airborne measurements were applied for providing additional information on meteorological parameters, especially for in-situ observations performed by UPS and KIT at Savè supersite. During field study, it turned out that the AE51 worked properly on board ALADINA and there was no loss of data. The large amount of 155 vertical profiles, including BC, is unique and led to further deeper analysis. After post-processing, the BC showed distinct layers in the vertical distribution, but could not be explained solely by the airborne data. The authors of TU Braunschweig decided to focus on the measured BC data, in particular for the case study on 14 and 15 July 2016 and were strongly supported by additional measurements conducted at Savè supersite (4 km distance).

This is the reason why filter samples of Savè supersite are used, although it has to be considered that these measurement methods are different and the calculated BC is not the same (here optical equivalent BC vs chemical analyses of BC). But, it is still the best way (or let’s say “a better first step”) to find possible sources or impacts of the clear distinct layers that were observed in the vertical distribution with ALADINA. The initial expectation was to identify any local emissions with the help of filter data. But there was no clear evidence of biomass burning in NOx or CO. Unfortunately, other BC measurements were lacking at the Savè supersite. rBC was measured with SP2 on manned aircraft (e.g. Flamant et al., 2018; Brito et al., 2018) but both measurement systems are not comparable due to sampling different air masses. The flight strategy of UAS is targeting small scale studies in contrast to large scale studies by manned aircraft with a fast cruising speed.

But, the large variability of BC in the lowermost 1 km could be better understood by the impact of the prevailing weather situation, shown with ceilometer and wind profiler. The study benefits from the comparison with COSMO-ART in order to get a broader perspective of BC transport, as all other instruments were running at Savè supersite, 4 km away from the research flights. Although the validation may look a bit odd, validated transcends definitely help to verify the source of long range transport of BC. Therefore, we decided to keep it. This may help to understand the decision of using the model output (referring to Comment RC1 3.).

However, during review process the study of Pikridas et al. (2019) was published that showed the comparison of three different miniaturised absorption instruments on UAS with ground based monitoring of MAAP and AE33. The AE51, a DWP (dual-wavelength prototype of AE51) and STAP were used on board three different types of UAS. Flights were carried out at an urban location (Athens) and at a background location in Cyprus. A direct comparison of each of the instrumentation was done at ground when no vertical profile was operated. In addition, a multicopter sampled between 2 and 3 min duration at ground level. The combination of samples was used for a direct- so called intercomparison- of the instrumentations. Some results of the Athens campaign: The correlation of AE51 and MAAP/AE33 was R^2=0.76, probably caused by the lower signal to noise ratio in contrast to the other sensors. BC mass concentrations were underestimated by 6 to 7% in relationship between MAAP and AE33. The comparison during the Cyprus campaign showed a high overestimation (22+/-55% EBC) of the AE51, possibly caused by low background concentration and low sampling flow. Interestingly, the comparison was done on a multicopter so that high vibrations of the rotor blades could probably influence the sampling flow as well, but the effect was not considered in the study. Nevertheless, the study offers a great opportunity for a better understanding of the AE51 signals on board in contrast with ground observation. The authors decided to include the study in the new manuscript in order to verify the capability of the micro aethalometer.

We added following lines to the new manuscript (marked up manuscript p. 7, l.13-25):

"However, a direct comparison of the AE51 on UAS relating to ground observations was missing so far. Pikridas et al. (2019) showed that the AE51 is a feasible tool for

BC measurements on UAS in an area of high background aerosol particle concentration. Flight campaigns were conducted in Athens and Cyprus. The results are based on comparison of three different miniaturised absorption instruments (e.g. AE51) on UAS with ground based monitoring of MAAP (Multi Angle Absorption Photometer) and one micro aethalometer of type AE33. According to results of the Athens campaign, the correlation of AE51 was R2=0.76 by sampling close to ground in relationship between MAAP and AE33. BC was underestimated by the AE51 of 6 to 7%, thus within the given accuracy of 10%. However, the comparison during the Cyprus campaign showed a high overestimation of 22–55% BC by the AE51, possibly caused by low background aerosol particle concentration at the research site. The low performance of the instrument for small background concentration in generally clean air masses is one major issue of the AE51 (e.g., Ferrero et al., 2014; Lee, 2019). The impact should be of minor relevance for the current study that addresses an area with high PM concentration, partially higher than WHO guidelines (Adon et al., 2019). However, during laboratory tests it became apparent that readings of the micro aethalometer are also sensitive to changes in temperature and humidity. This will be further addressed."

RC1: *"The authors mention, at the bottom of page 4, that the accuracy of the microaethelometer was tested in the lab. This work should be presented fully in this paper as it speaks directly to the reliability of this data."*

Authors' response:

The authors refer to laboratory tests that were performed in a temperature chamber after the campaign. The tests were done in order to characterise/understand the cause of temperature artefacts. We agree that this should be pointed out in a clearer way. It was assumed that temperature error was the main impact on the BC readings during the DACCIWA study.

Changes in the manuscript are provided in the answer to the next comment.

RC1: *"2. Along similar lines, I am very concerned about the temperature correction. As shown it appears to be a 3 ug/m3 correction for a change of 8C? Unless I'm* *misunderstanding that figure and associated discussion that is a huge correction factor. The correction is then bigger than most of the measurements. I can't even imagine what would cause the measurement to be temperature sensitive. Is it the light source? That would be a big change in intensity. Much more needs to be said about this. For example, is the case shown the worst-case scenario in terms of a flight with a strong temperature profile or is that typical? I think the authors should show the vertical profile of the correction factor. At a minimum, some discussion should be added describing the frequency with which large temperature corrections were applied and addressing the question of how errors in this correction factor might affect the interpretation presented here."*

Authors' response:

Indeed, we were also a bit shocked about the temperature gradient error. Although we made intense tests in the climate chamber, we could not determine the exact source of the error. One assumption could be the load of the optical part (light source/detector/reference measurement). Errors were reproducible, but the study of these errors would ask for its own paper, since many measurements and discussions rely on the AE51 in the range of these errors. Probably the description of data treatment is misleading or not understandable in the manuscript (old version p. 5, l. 27-28). "For the whole study, the BC data were corrected with the internal temperature changes measured directly at the BC sensor."

Now, we will describe it more in detail:

The correction factor was used for the analysed BC data (all flights and all vertical profiles). The sharpest temperature gradients were observed at the beginning of the A51 sampling, prior to take-off. The strong heating could be in relation to inner warming of the UAS when it was prepared for the next flight at the airfield (high incoming solar radiation).

The worst case scenario was shown in Fig. 4.; in most cases the temperature gradients were significantly smaller for the rest of the study. We agree that pointing out the worst case would be at least the minimum information! However, the large temperature gradients at the beginning of the flights do not influence the results of the study. For further information: the high impact does not affect the calculated ascents/descents, shown in the vertical profiles in Fig. 11.

The take-off of the UAS is handled by the safety pilot with remote control and we exclude the first parts of the flight mission due to irregular flight sections (mostly between surface and 100 m) that could not be used for the wind measurements (in-flight calibration etc). Therefore, the extreme parts were not considered, but we always took into account the bias of 0.25 µgBC/(dT/dt)$^{-1}$, calculated from the lab.

Nevertheless, we totally agree that the AE51 still needs more profound understanding in the field in terms of appropriateness!

We changed the paragraph to (marked up manuscript p. 7, l. 27- p.8, l. 10):
“As example, the impact of temperature changes on the attenuation is shown for a flight that was performed with ALADINA on 14 July 2016 (flight ID 41 of 53 total measurement flights). Figure 2 presents the internal temperature from the micro aethalometer (PCBtemp) during the measurement period from 05:16 until 06:30 UTC that varied between 27 and 36 °C. This flight was chosen as the worst case scenario during the study. In order to determine the temporal evolution of temperature, the bit noise has to be filtered out by any smoothing algorithm. Taken from laboratory tests in a temperature chamber, the influence factor of temperature changes on BC measurements was determined to be in the order of 0.25 µgBC (dT/dt)$^{-1}$. Applied for the current case, largest temperature gradients were observed between 05:16 and 05:30 UTC during the first steps of the ascent, leading to a bias (shown in BC Error, lower panel of Fig. 2) of 3 µg BC/m³. BC data were corrected with the internal temperature changes measured directly at the BC sensor for the whole study. Here, it should be clarified that these first steps of ascent, and similar to all other flights, do not directly affect the here presented analysis. These first steps correspond to take-off that is handled in remote control by the responsible pilot. However, exclusively automatic flight tracks were used in order to obtain comparable vertical profiles and neglecting horizontal patterns. One possible cause of these large temperature gradients might be internal heating of the aircraft. During landing and preparation of the next research flight, the aircraft was exposed directly to sunlight. Another effect that could lead to this high BC error might be the load of the optical part. The error was reproducible in the laboratory, but the exact source of the error could not be determined. More tests in field studies would be mandatory.”

RC1: *“3. The comparison to the model is a bit odd. I can understand the value of comparing measured to modeled values but the way this analysis is written the model seems to be assumed to be correct rather than really evaluated. While I’m not sure that I’d call the AE51 “ground truth” I also doubt that the model is perfect and it seems like a stretch to me to rationalize model-measurement disagreement as artifacts. I’m not an expert in this field so I may not be aware of the literature but, have the emissions been fully validated? Has the aging scheme been compared to at least a handful of parallel observations? Have the modeled size distributions been validated? 20- 25% of the BC mass in the Aitken mode seems like a lot and it seems like the model didn’t represent the boundary layer very well (in that model concentrations seem to fall off while measurements are largely flat as a function of height). In the discussion of local vs advected emissions, four reasons are given. Two are purely model based and not convincing (the model shows that the feature is regional, the model predicts mostly aged emissions). The third sounds reasonable (NOx and CO don’t indicate local emissions) but those measurements should be shown and this should probably be the primary reason that advection is hypothesized. I don’t really understand the 4th reason. Are there big cities or other BC sources between the sampling location and the coast? Otherwise I don’t see how a seabreeze can bring both polluted air and clean air.”*

Authors’ response

The intention of the authors was to understand possible sources of enhanced BC layers in the boundary layer. Indeed, neither AE51 data nor model should be said as “ground truth”, but the validation benefits from the comparison in the vertical distribution. This is a very important point, as filter data is only reproducible at ground where no local emission was identified. Therefore, the data was only summarised in Tab. 1. But, a comparison of model with CO was presented in the dissertation of Deetz (2018) for the field campaign. COSMO-ART was compared with other models and with aircraft campaign during DACCIWA. As the full description of the model is not in the scope of the paper, we refer to the dissertation and another study of COSMO-ART by Deetz et al. (2018).

Further, Deroubaix et al. (2019) studied the diurnal cycle of NO and CO at Savè supersite between 1 and 7 July 2016. Low concentrations led to the assumption of transport processes that could be explained by tracer experiments from possible city plumes near the coast. We will refer to the reference in the conclusion in order to clarify the assumption of polluted air masses. In addition, we have made a new order of three hypotheses, as number 1 was not shown in this article it was removed.

The authors added following lines to the new manuscript (marked up manuscript p. 16, l. 14-18):
"This hypothesis can be supported by tracer experiments of Deroubaix et al. (2019), who showed that Savè is partly influenced by city plumes near the coast, namely Lomé, Accra and Cotonou due to maritime inflow from south. The modelled period was 1–7 July but the conditions of the vortex phase on 14 July 2016, unusual during the monsoon season, included transport of aged biomass burning aerosol and decreased humidity, as described in Knippertz et al. (2017) and Flamant et al. (2018) so that long range transport from city plumes might be the source of observed BC in Savè."

References:

- Deetz, K. (2018). Assessing the Aerosol Impact on Southern West African Clouds and Atmospheric Dynamics, Environmental Science, DOI:10.5445/IR/1000081308.

- Deetz, K., Vogel, H., Haslett, S., Knippertz, P., Coe, H., and Vogel, B.: Aerosol liquid water content in the moist southern West African monsoon layer and its radiative impact, Atmos. Chem. Phys., 18, 14271–14295, https://doi.org/10.5194/acp-18-14271-2018, 2018.

- Deroubaix, A., Menut, L., Flamant, C., Brito, J., Denjean, C., Dreiling, V., Fink, A., Jambert, C., Kalthoff, N., Knippertz, P., Ladkin, R., Mailler, S., Maranan, M., Pacifico, F., Piguet, B., Siour, G., and Turquety, S.: Diurnal cycle of coastal anthropogenic pollutant transport over southern West Africa during the DACCIWA campaign, Atmos. Chem. Phys., 19, 473–497, https://doi.org/10.5194/acp-19-473-2019, 2019.

Smaller issues of RC1

RC1: *"1. There are some language issues, especially towards the beginning, and I recommend English language editing. "If BC is once emitted" should be "Once BC is emitted". In the same sentence there are several unnecessary "thes", a problem which appears throughout. There are many instances where the sentence construction and grammar make it hard to understand what the authors are saying.*

Authors' response:

Thank you very much for the hint. As described above, we will take into account English language editing for the revised manuscript. Then, the manuscript should be clearer in its aim. Unnecessary "thes" were avoided in order to simplify the reading flow.

RC1: *"2. A smaller comment with regard to the data processing of the aethalometer. I don't really know what "phase shift free low pass" filtering is. The noise looks fairly random. Why not use a simple average to deal with the noisiness of the high time resolution data?"*

Authors' response:

A moving average inherits a poor frequency response (poor stopband attenuation and slow roll-off). Therefore, we use a Butterworth IIR-Filter running forward and backward to eliminate phase shifts.

The explanation was added to the manuscript (marked up manuscript p. 8., l. 12-13): "Therefore, a high-pass Butterworth filter of third order was used, running forward and backward to eliminate phase shifts Averaging was not applied for the attenuation signal in avoidance of poor frequency responses."

RC1: "*3. I'm unsure of your meaning in Line 21 with regard to hygroscopic growth. Why does hygroscopic growth enable coating?"*

Authors' response:

The authors agree that this is a really misleading sentence. The intention was to emphasise the role of BC after a long residence time in the atmosphere that is ongoing with a hygroscopic growth and the CCN activity is increased by a possible coating with other species. The sentence is rephrased and simplified.

The sentence is now (marked up manuscript p. 2, l. 5-7): "Aged BC can act as cloud condensation nuclei after hygroscopic growth in the atmosphere (Zhang et al., 2008), which ultimately contributes to the indirect aerosol effect".

RC1: *"4. There are already a lot of figures for a relatively brief paper. I don't see the value in including the power spectra graphs for the wind vectors. There you could just refer to previously published reports of that payload, especially since the present analysis doesn't seem to make use of high-resolution wind products."*

Authors' response:

Thank you a lot for the hint. We agree that the publication involves a lot of figures and the first part might distract from the results. In order to focus more on the results, the authors will remove Fig. 1 and Fig. 3. Figure 2a displays the measurement unit, including the meteorological sensors and Fig.2b shows the integration of the AE51 in the UAS. As these instrumentations were used for the study, it would not be mandatory to show the aircraft itself. We will only refer to previous publications of Altstädter et al. (2015) and Bärfuss et al. (2019). Turbulence was not calculated for the shown BC study, so that Fig. 3 will be withdrawn, as well.

RC1: *"5. In figure 8, I recommend that you change the x-axis label in the upper right panel to say "water mixing ratio" rather than just "mixing ratio"."*

Authors' response:

Thank you, this is an important issue. The authors will change the label of the x-axis, accordingly. This will be done for Fig. 8, Fig. 11 and Fig. 12 of the old manuscript, as well.

RC1*: "6. In figure 12 you label one line as "wash out". This term is also used in the conclusions but not in the discussion. What do you mean by this? Are the low level clouds precipitating or is it just that cleaner air blew in? If it's the latter I wouldn't call that wash out, I would call it advection of cleaner air."*

Authors' response:

The term "wash out" was removed from Fig. 12, as it might have led to misleading interpretation. The authors' intention was to highlight the decreasing BC in the lowermost 350 m after the onset of low-level clouds. We do not have any evidence, if the cause of the removal was wash out or just the transport of a generally cleaner air mass.

RC1: *"7. On the wind plots, how is the direction indicated by the arrows? I'm used to seeing these plotted on graphs with lat-lon as the axis but I'm not sure they make sense plotted on axes of height-time. I imagine you are just showing direction where N is "up" so perhaps the solution is to simply include a legend showing that? It's kind of an awkward graphic but I don't have a great solution for it."*

Authors' response:

Thank you for the hint. We should add more information on wind arrows. A shown leftwards horizontal arrow presents a wind direction from E. An arrow from bottom to top stands for S wind. We decided not to change the figure, but to include the information in the capture of Fig. 10, like it was done in other results of wind profiler measurements during DACCIWA (e.g. Dione et al., 2019).

RC1: *"8. There are a number of acronyms that are only used a handful of times. Notable NLLJ and LLC. Given the frequency of usage I recommend that, those just be written in full."*

Authors' response:

Ok thank you for the hint. The authors decided to use the full expressions for those which are only used for a few times.

Author's response to referee #2

Point-to-point response:

RC2: *"This paper presents aethalometer measurement from the field experiment DACCIWA conducted in the atmospheric boundary layer in Benin. The campaign is interesting and conducted in a region where better observational coverage is needed, and black carbon in the boundary layer is interesting for a number of reasons. The paper hence provides a topical contribution to the field. However, in my opinion the manuscript needs substantial additional work to improve presentation, message and context. General comments: While results are presented clearly and in great detail, I'm struggling to identify and capture the main messages of the study. For instance, the "Conclusion" section does not really provide any conclusions or outlooks, and the paper does not contain much in terms of discussion of relevance of results from a broader perspective."*

Similarly, a bit more context in terms of why these measurements are important would be useful. E.g., the introduction could focus a bit more explicitly on the importance of BC in the boundary layer in terms of disturbances to turbulence, citing some recent studies such as Wilcox et al. (PNAS, 2016), Talukdar et al. (2019, JGR-atmospheres), Liu et al. (Atmospheric Pollution Research 2018), Gao et al. (ACP 2018)."

Authors' response:

The authors thank the anonymous referee for proof reading and for the specific comments that will improve the current manuscript. We agree that the previous manuscript did not point out clear enough the main massage of the study. The goal is to link between surface observations and airborne measurements within the boundary layer in the West African monsoon area, supporting the aim of DACCIWA. In this study, surface observations were used for a characterisation of gas concentrations and the upper part of the atmosphere was described with the help of wind profiler and ceilometer data.

Please see the answers at p.1. We have fully revised the abstract and conclusions to point out the main goal of study.

The abstract is now (marked up manuscript p. 1, l. 1-23):

"This study underlines the important role of transported black carbon (BC) mass concentration in the West-African Monsoon (WAM) area. BC was measured with a micro aethalometer integrated in the payload bay of the unmanned research aircraft ALADINA (Application of Light-weight Aircraft for Detecting IN situ Aerosol). As part of the DACCIWA (Dynamics-Aerosol-Chemistry-Cloud Interactions in West Africa) project, 53 measurement flights were carried out at Savè, Benin, in 2–16 July 2016. A high variability of BC (1.79 to 2.42 +/- 0.31 $\mu g/m^3$) was calculated along 155 vertical profiles that were performed below cloud base in the atmospheric boundary layer (ABL). In contrast to initial expectations of primary emissions, the vertical distribution of BC was mainly influenced by the stratification of the ABL during the WAM season. The study focuses on an event (14 and 15 July 2016), which showed distinct layers of BC in the lowermost 900 ma bove ground level (a.g.l.). Low concentrations of NOx and CO were sampled at Savè supersite near the aircraft measurements and suggested low impact of local sources during the case study. The lack of primary BC emission was verified by a comparison of the measured BC with the model COSMO-ART (Consortium for Small-scale Modelling–Aerosols and Reactive Trace gases) that was applied for the field campaign period. The modelled vertical profiles of BC led to the assumption that the measured BC was already altered, as the size was mainly dominated by the accumulation mode. Further, calculated vertical transects of wind speed and BC presume that the observed BC layer was transported from south with maritime inflow, but was mixed vertically after to the onset of a nocturnal low-level jet at the measurement site. The study contributes to the scope of DACCIWA by linking airborne BC data with ground observations and model and it illustrates the importance of a more profound understanding of the interaction between BC and the ABL in the WAM region."

The conclusion was changed to (marked up manuscript p. 15, l. 4-p. 16, l. 23):

"This article aims at understanding the relationship between the vertical distribution of BC in the ABL in southern West-Africa. The investigation area is supposed to be one of the major sources for BC emissions worldwide (Liousse et al., 2014). But where do those BC emissions originate, especially in the ABL? Beyond surface measurements, the role of BC is difficult to assess within the ABL due to lacking column measurements. ALADINA was applied for meteorological profiling and BC measurements during the extensive field experiment of DACCIWA at Savè, Benin, in 2–16 July 2016. BC was measured with a micro aethalometer, model AE51, that has been proved as feasible tool on UAS, but it suffers from artefacts that were one subject of this paper. Prior to analyses, BC data were corrected with bias caused by the dependence of the instrumentation on internal temperature during ascents and descents. Further, a low pass filter was applied for the readings with a resolution of 10 s.

For a statistical overview, BC was averaged for altitude intervals of 20m steps along 155 vertical profiles of the whole measurement period. In contrast to initially expectations, no clear influence of primary BC emission was observed in the vertical distribution. It was shown that BC occurred in the whole ABL and did not decrease depending on the altitude. Thus, maxima and minima of BC concentration could be caused by other aspects than solely from ABL conditions. One explanation could relate to horizontal advection processes that might have brought about different types of air masses with distinguished layers of BC. Another explanation could be based on regional-scale. The measurement period was influenced by the WAM season, leading to high occurrence of nocturnal low-level jet and low-level clouds that could have strongly affected the vertical distribution of BC due to dynamics in the ABL. (e.g., Dione et al., 2019; Kalthoff et al., 2018; Adler et al., 2019; Babic et al., 2019a).
One case study (14–15 July 2016) was presented in detail in order to clarify possible other impacts on the BC distribution. Therefore, ground observations of wind profiler, ceilometer and gas concentrations were used from Savè supersite, 4 km away from the research flights. NOx and CO did not show any clear evidence of local emissions at ground. However, a maximum of BC=2.81 +/- 0.30 µg/m³ was observed in the residual layer between the heights of 400 and 600 m a.g.l. in relation to a nocturnal low-level jet with wind speeds larger than 12 m/s. The lifted BC layer was vertically mixed during clear sky conditions during the day and the mass concentration increased continuously in the lowermost 1100 m a.g.l. On the next day, low-level clouds formed in the early morning that might have led to wash out in the lowermost 400 m a.g.l. BC decreased from 3.87 +/- 0.79 to 2.51 +/- 0.13 µg/m³ in the same altitude. The UAS observations were supported and spatially extended by a comparison with the model output of COSMO-ART during the event. In all cases, the

contribution of fresh BC to the total BC was negligible in COSMO-ART, indicating that local sources were not the major contributor of BC over Savè. The analysis of longitudinal vertical transects of the modelled wind speed and the BC mass concentrations revealed that transport processes with maritime inflow from the south could be the most relevant contributors of the observed BC.

This hypothesis can be supported by tracer experiments of Deroubaix et al. (2019), who showed that Savè is partly influenced by city plumes near the coast, namely Lomé, Accra and Cotonou due to maritime inflow from south. The modelled period was 1–7 July but the conditions of the vortex phase on 14 July 2016, unusual during the monsoon season, included transport of aged biomass burning aerosol and decreased humidity, as described in Knippertz et al. (2017) and Flamant et al. (2018) so that long range transport from city plumes might be the source of observed BC in Savè.

The strength of the shown study is the high capability to further understand transport processes of BC on small-scale by using UAS that are linked to regional-scale during the WAM season.

However, the relationship between BC and the ABL needs more profound investigations. In addition, the impact of possible aged and transported BC within the ABL should be taken into account in future investigations that could equally contribute to a reduction of air quality and even further interact with low-level clouds.”

Thank you very much for providing the current literature! We included the study of Wilcox et al. (2016) and Liu et al. (2018) in the introduction. The references allow a more concrete analysis of the ABL height and its interaction with BC.

Following lines were added to the new manuscript (marked up manuscript p. 3, l. 5-35):

“However, previous data showed only the large scale variability of BC instead of columns on smaller scales of a few square kilometres above one concrete measurement field. In particular the relationship between the ABL and BC distributions needs more profound investigations. Liu et al. (2018) studied the ABL height for 347 days depending on the classification of polluted (BC>5 μg/m³) and non-polluted events (BC<5 μg/m³) in Wuhan, China. The ABL height was suppressed on polluted days, which ultimately leads to poorer air quality. The reduction of the ABL height can be explained by the increase of absorption due to enhanced particulate matter originating from pollution (e.g., Petäjä et al., 2016). The growing absorption heats up the upper part of the ABL which further results in an increase of stability. As cause of weaker turbulence and mixing in more stable conditions, the ABL height decreases. But in most investigations, BC is solely measured at ground. Further, Liu et al. (2018) calculated the top of the ABL from lidar measurements neglecting cases with low clouds. So that studies are missing with non-clear sky days like during monsoon seasons.

Therefore, a large benefit can be expected by using unmanned aerial systems (UAS) for investigating the small scale variability of BC in the ABL. Relating to BC measurements, optical methods based on light-absorbing principle are common. The development of miniaturised BC instrumentation is essential, as reduced size and limitation of weight are the main challenges of new sensor integration on airborne platforms. Wilcox et al. (2016) presented vertical profiles of BC, measured with a miniaturised three wavelength absorption photometer (Corrigan et al., 2008) on UAS, during the winter monsoon over the northern Indian Ocean. BC loads were higher in the lowermost 3 km on polluted days in comparison with days of minor pollution observed at the surface. A lower ABL height was estimated during polluted days, supporting the current understanding of feedback mechanisms, like it was summarised in Petäjä et al. (2016). However, the observations showed an increase of humidity in the surface mixed layer that might favour cloud formation that is in contrast to the understanding of a lower instability and minor turbulence due to absorption of aerosols in the ABL. Thus, further studies are essential to better understand the role of BC in the ABL and to consider potentially other impacts on the vertical distribution in a broader range."

RC2: *"The language needs to be reviewed and improved. There are a number of somewhat strange and incorrect sentence structures, making the manuscript difficult to follow. And a lot of unnecessary "the"s. Some of the acronyms would be better to spell out."*

Authors' response:

The authors agree that the language should be revised in order to avoid any misleading interpretations. Unnecessary "thes" were removed and the acronyms are provided in full. Please, see comments above on the first page and the answers to the first referee.

RC2: *"More specific comments: I think the authors should use the recommendations from Petzold et al. 2013 regarding terminology for reporting measurements of "black carbon" and use EBC here (or at least be clear that the term BC is used as a generic term)."*

Authors' response:

We are grateful for your recommendation. The comparison of different measurement methods is still an important issue, as the BC strongly differs in its properties. We have added the following lines in the aethelometer section. We decided not to refer to the recommendation in the introduction, as the introduction presents the role of BC in general.

We made following change (marked up manuscript p. 6., l. 14-21):
"Further, it has to be considered that different measurement methods (for instance optical or chemical) lead to different types of BC. A clear terminology is mandatory (Petzold et al., 2013). In terms of the presented study, the equivalent black carbon (EBC) was calculated from the light-absorbing aethalometer. Only for the sake of simplicity, the term BC will be used hereafter."

RC2: *"On page 3, it is pointed out that the conditions during the selected cases are unusual for the monsoon period. What does this imply for the representativeness and usefulness of these results?"*

Authors' response:

In our opinion, the unusual monsoon period affected the long range transport of BC. Decreased humidity might have caused a degradation of wet deposition.

Nevertheless, the comment is not helpful in the introduction and it was postponed to the conclusion.

RC2: *"Suggest combining Figures 1 and 2 as the paper already contains a large number of plots."*

Authors' response:

Thank you very much for the hint. We have removed Fig. 1 and Fig. 3 in order to reduce the amount of figures. Figure 2 is sufficient, as we only focus on the measurement unit. Figure 3 was withdrawn, because we did not use turbulence data for the study.

RC2: *"Section 2.3.1: a brief introduction to this section about what causes this temperature effect would be very useful for non-experimentalist readers."*

Authors' response:

Yes, indeed. We have added the information on temperature gradient error. We assume the load of the optical part for a possible cause. However, although the error was reproducible in the lab, the exact source of the error could not be determined; more tests in field studies would be mandatory.

RC2: *"Page 6, line 3: how is "acceptable" defined?"*

Authors' response: The frequency response will be lost by a span of 30 sec or more. Thus, 10 sec will still reproduce the high noise of the attenuation signal in order to capture possible enhanced BC loads in the vertical distribution. In the shown case, the term of "acceptable" noise refers to standard deviation smaller than 0.3 µg/m³ (22 %) of the signal.

RC2: *"Section 2.4: A brief description about the parameterizations of wet and dry removal of the aerosols would be useful."*

Authors' response:

It is beyond the scope of this publication to give detailed information on numerical simulations. The parameterizations of processes are provided in Deetz (2018) and Deetz et al. (2018).

RC2: *"Page 6, line 31: does the presence of dry and sandy soils present a source of uncertainty in the measurements?"*

Authors' response:

The presence of dry and sandy soil was a major issue due to possible damages during take-off and landing for the meteorological sensors, as they are mounted at the tip of the aircraft's nose. However, the housings over the finewire-sensor were reliable and none of the sensors had to be replaced. The impact of dust particles on the airstream could definitely affect the sampled flow. However, no tests were performed at the measurement site. We can only guess if the filter load could be affected by the dust particles. In order to avoid any contamination during test procedures at ground, the sample flow was filtered at the inlet. In our opinion, the impact of dust particles that could be entering the inlet during take-off should be negligible in the attenuation signal (due to the scattering properties of dust) but could have led to stronger loading on the optical part. Dust particles present continuously on the filter should not affect the measurements, as the incremental changes of the optical properties are used to derive the BC mass concentration.

RC2: "Page 10, lines 15-17: please check the use of "on one hand (. . .). On the other hand

(. . .)". **RC2:** ***"****Page 10, lines 178-19: as the observations do not allow for an investigation of evolution*

of mixing state, I don't quite see why this information is included."

Authors' response:

The authors combined both remarks of the second referee hereafter. We decided to change this paragraph about the model, as the mixing of BC is not relevant for the aethalometer measurements of the shown study. The initial assumption of the sharp gradients of the measured BC in the vertical distribution was the observation of activated BC, as the flights were performed near clouds or close to the edge of clouds. However, we assume that turbulence near cloud base and probably cloud droplets disturbed the inflow and led to high BC artefacts. Nevertheless, the model still provides helpful information on the source of the aged BC properties.

RC2: "*Page 11, line 3: this statement seems a bit odd – you'd want the observed profile to agree with total modeled BC. Individual size modes may be important for discussion of why the discrepancy with total BC is there."*

Authors' response: Thank you very much. The intention was not to state which of the methods is the right one. The sentence was rephrased and possible explanations were added to the text.

The authors made this change (marked up manuscript p. 14, l. 4-10):

"At 06:00 UTC on 15 July 2016 (see Fig.11e) observation and model indicate an enhanced BC concentration below 400 m a.g.l. The vertical profile, capturing the lowest 900 ma.g.l., shows a representative agreement of observation and model of total BC. Around the height of 200 m a.g.l., ALADINA indicates high BC concentrations of more than 16 µgm³ that are not represented in COSMO-ART. The discrepancy could be based on the 1 s sampling of ALADINA that is strongly noisy. The first assumption was turbulent mixing near the cloud edge that might have led to high variability of the sampling flow, thus on BC data. Another possibility could be droplets that disturbed the signal. However, it cannot be ruled out that this is an artefact induced by high humidity prior to the onset of cloud formation, which occurred around that time."

Authors’ changes

Please take into account some additional changes of the authors.

The references of Babić et al. (2019), Dione et al. (2019) and Pacicifo et al. (2019) were revised during the review process of this manuscript.

- Babić, K., Kalthoff, N., Adler, B., Quinting, J. F., Lohou, F., Dione, C., and Lothon, M.: What controls the formation of nocturnal low-level stratus clouds over southern West Africa during the monsoon season?, Atmos. Chem. Phys., 19, 13489-13506, https://doi.org/10.5194/acp-19-13489-2019, 2019.
- Dione, C., Lohou, F., Lothon, M., Adler, B., Babić, K., Kalthoff, N., Pedruzo-Bagazgoitia, X., Bezombes, Y., and Gabella, O.: Low-level stratiform clouds and dynamical features observed within the southern West African monsoon, Atmos. Chem. Phys., 19, 8979–8997, https://doi.org/10.5194/acp-19-8979-2019, 2019.
- Pacifico, F., Delon, C., Jambert, C., Durand, P., Morris, E., Evans, M. J., Lohou, F., Derrien, S., Donnou, V. H. E., Houeto, A. V., Reinares Martínez, I., and Brilouet, P.-E.: Measurements of nitric oxide and ammonia soil fluxes from a wet savanna ecosystem site in West Africa during the DACCIWA field campaign, Atmos. Chem. Phys., 19, 2299–2325, https://doi.org/10.5194/acp-19-2299-2019, 2019.

Additional literature was used for the new manuscript.

- Adon, A. J., Liousse, C., Doumbia, E. T., Baeza-Squiban, A., Cachier, H., Léon, J.-F., Yoboue, V., Akpo, A. B., Galy-Lacaux, C., Zoutien, C., Xu, H., Gardrat, E., and Keita, S.: Physico-chemical characterization of urban aerosols from specific combustion sources in West Africaat Abidjan in Côte d’Ivoire and Cotonou in Benin in the frame of DACCIWA program, Atmos. Chem. Phys. Discuss., https://doi.org/10.5194/acp-2019-406, in review, 2019.
- Altstädter, B., Platis, A., Jähn, M., Baars, H., Lückerath, J., Held, A., Lampert, A., Bange, J., Hermann, M., and Wehner, B.: Airborne observations of newly formed boundary layer aerosol particles under cloudy conditions, Atmos.

Chem. Phys., 18, 8249–8264, https://doi.org/10.5194/acp-18-8249-2018, 2018.

- Corrigan, C. E., Roberts, G. C., Ramana, M. V., Kim, D., and Ramanathan, V.: Capturing vertical profiles of aerosols and black carbon over the Indian Ocean using autonomous unmanned aerial vehicles, Atmos. Chem. Phys., 8, 737–747, https://doi.org/10.5194/acp-8-737-2008, 2008.
- Deetz, K., Vogel, H., Haslett, S., Knippertz, P., Coe, H., and Vogel, B.: Aerosol liquid water content in the moist southern West African monsoon layer and its radiative impact, Atmos. Chem. Phys., 18, 14271–14295, https://doi.org/10.5194/acp-18-14271-2018, 2018.
- Deroubaix, A., Menut, L., Flamant, C., Brito, J., Denjean, C., Dreiling, V., Fink, A., Jambert, C., Kalthoff, N., Knippertz, P., Ladkin, R., Mailler, S., Maranan, M., Pacifico, F., Piguet, B., Siour, G., and Turquety, S.: Diurnal cycle of coastal anthropogenic pollutant transport over southern West Africa during the DACCIWA campaign, Atmos. Chem. Phys., 19, 473–497, https://doi.org/10.5194/acp-19-473-2019, 2019.
- Lee, J.: Performance Test of MicroAeth® AE51 at Concentrations Lower than 2 μgm□3 in Indoor Laboratory, Appl. Sci., 9, 1–14, doi:10.3390/app9132766, 2019.
- Liu, B., Ma, Y., Gong, W., Zhang, M., and Shi, Y.: The relationship between black carbon and atmospheric boundary layer height, Atmos. Pollut. Res., 10, 65-–72, https://doi.org/10.1016/j.apr.2018.06.007, 2018.
- Platis, A., Altstädter, B., Wehner, B., Wildmann, N., Lampert. A., Hermann, M., Birmili, W., and Bange, J.: An observational case study on the influence of atmospheric boundary layer dynamics on the new particle formation, Bound.-Lay. Meteorol., 158, 67–92, doi:10.1007/s10546-015-0084-y, 2016.
- Petäjä, T., Järvi, L., Kerminen, V. M., Ding, A. J., Sun, J. N., Nie, W., Kujansuu, J., Virkkula, A., Yang, X., Fu, C. B., Zilitinkevich, S., and Kulmala, M.: Enhanced air pollution via aerosol-boundary layer feedback in China, Sci. Rep., 6, 18998, doi:10.1038/srep18998, 2016.
- Petzold, A., Ogren, J. A., Fiebig, M., Laj, P., Li, S.-M., Baltensperger, U., Holzer-Popp, T., Kinne, S., Pappalardo, G., Sugimoto, N., Wehrli, C., Wiedensohler, A., and Zhang, X.-Y.: Recommendations for reporting "black

carbon" measurements, Atmos. Chem. Phys., 13, 8365-8379, https://doi.org/10.5194/acp-13-8365-2013, 2013.

- Pikridas, M., Bezantakos, S., Močnik, G., Keleshis, C., Brechtel, F., Stavroulas, I., Demetriades, G., Antoniou, P., Vouterakos, P., Argyrides, M., Liakakou, E., Drinovec, L., Marinou, E., Amiridis, V., Vrekoussis, M., Mihalopoulos, N., and Sciare, J.: On-flight intercomparison of three miniature aerosol absorption sensors using unmanned aerial systems (UASs), Atmos. Meas. Tech., 12, 6425–6447, https://doi.org/10.5194/amt-12-6425-2019, 2019.
- Wilcox, E. M., Thomas, R. M., Praveen, P. S., Pistone, K., Bender, F. A., and Ramanathan, V.: Black carbon solar absorption suppresses turbulence in the atmospheric boundary layer, P. Natl. Acad. Sci. USA, 113, 11794-11799, https://doi.org/10.1073/pnas.1525746113, 2016.

After changing the discussion and conclusion, some literature was removed. To the current knowledge of the authors, the study of Bessardon et al. (2018) was not resubmitted so far, so that it was withdrawn as well in the new manuscript.

- Adler, B., Kalthoff, N., and Gantner, L.: Nocturnal low-level clouds over southern West Africa analysed using high-resolution simulations, Atmos. Chem. Phys., 17, 899–910, doi:10.5194/acp-17-899-2017, 2017.
- Bessardon, G., Brooks, B., Abiye, O., Adler, B., Ajao, A., Ajileye, O., Altstädter, B., Amekudzi, L. K., Aryee, J. N. A., Atiah, W. A., Ayoola, M., Babi´c, K., Bärfuss, K., Bezombes, Y., Bret, G., Brilouet, P.-E., Cayle-Aethelhard, F., Danuor, S., Delon, C., Derrien, S., Dione, C., Durand, P., Fosu-Amankwah, K., Gabella, O., Groves, J., Handwerker, J., Kalthoff, N., Kohler, M., Kunka, N., Jambert, C., Jegede, G., Lampert, A., Leclercq, J., Lohou, F., Lothon, M., Medina, P., Pätzold, F., Pedruzo Bagazgoitia, X., Reinares, I., Sharpe, S., Smith, V., Sunmonu, L. A., Tan, N., andWieser, A.: A dataset of the 2016 monsoon season meteorology in southernWest Africa – an overview from the DACCIWA campaign, Sci. Data, in review, 2018.

- Gounou, A., Guichard, F., and Couvreux, F.: Observations of diurnal cycles over a West African meridional transect: Pre-monsoon and full-monsoon seasons, Bound.-Layer Meteor., 144, 329–357, doi:10.1007/s10546-012-9723-8, 2012.
- Hannak, L., Knippertz, P., Fink. A. H., Kniffka, A., and Pante, G.:Why Do Global Climate Models Struggle to Represent Low-Level Clouds in the West African Summer Monsoon?, J. Climate, 30, 1665–1687, doi:10.1175/JCLI-D-16-0451.1, 2017.
- Hansen, J., Sato, M., and Ruedy, R.: Radiative forcing and climate response, J. Geophys. Res., 102, 6831–6864, doi:10.1029/96JD03436, 20, 1997.
- Knippertz, P., Fink, A. H., Schuster, R., Trentmann, J., Schrage, J. M., and Yorke, C.: Ultra-low clouds over the southern West African monsoon region, Geophys. Res. Lett., 38, L21808, 1–7, doi: 10.1029/2011GL049278, 2011.

The statistical results were added by following lines in order to describe the possible impact of BC in the ABL (marked up manuscript p. 11, l. 18-31).

“All mean values showed a sharp gradient at the height of 600 ma.g.l. One explanation for this could be less data availability above this height. The research flights are restricted below cloud base, as ALADINA is not rain proof. The first part of the measurement period (2-8 July 2016) was during the post-onset phase of the WAM season (Knippertz et al., 2017). This period was influenced by low-level clouds with a median height of cloud top at 587 ma.g.l., taken from 06:00 UTC radiosondes at Savè (Kalthoff et al., 2018). This part corresponds to almost half (25 of 53) of the research flights. Although, nocturnal low-level clouds dissolved during the day, a large portion of vertical profiles still remained below 600ma.g.l. Drier periods occurred during the vortex phase of the WAM that was predominant from 9 until 17 July 2016 (Knippertz et al., 2017). Taken from the statistic overview of BC, BC seems to occur in the whole ABL. No clear evidence is visible of local pollution near surface. One explanation could be the performance of ALADINA during daytime so that in some cases the ABL was already well mixed and BC was lifted from ground through the ABL. However, this can not be supported by mean theta that shows an overall stable ABL. This relationship presumes that observed BC originated prior to the observation periods, probably during night or even earlier. Another possibility could be horizontal advection that caused distinguish layers of BC in the ABL. Here, the understanding of BC in the ABL can not be fully described by previous observations like Wilcox et al. (2016) and Liu et al. (2018). Directly emitted BC would have probably warmed the ABL by absorption that further caused stable conditions and a lower ABL height but with increased humidity. This is in contrast to here observed reduced humidity due to the decline of mean q in the ABL. Therefore, it is essential to take into account other aspects that might affect the BC distribution within the ABL."

The paragraph of using UAS for ABL studies was removed from the introduction to the ALADINA section (marked up manuscript p. 4, l. 21-27):

"There is a wide range of airborne platforms, including UAS operating with batteries and fuel engines, both fixed wings and multicopters that are applied for atmospheric research on a various sampling locations (e.g., Mayer et al., 2010; Marino et al., 2015; Renard et al., 2016; Jiménez et al., 2016; Cuxart et al., 2016; Båserud et al., 2016; Brosy et al., 2017). The different systems have advantages and shortcomings. In terms of ALADINA, the aircraft is electrically powered, so that any contamination of the measured air probe can be prevented. Thus, a qualitative analysis of aerosol particles is guaranteed by sampling in short periods of time, like it was done in previous studies of ALADINA (Platis et al., 2016; Altstädter et al., 2018) in Melpitz, Germany."

Additional information of instrumentation on ALADINA was provided (marked up manuscript p. 5, l. 10-14):

"Other aerosol sensors (optical particle counter and condensation particle counter) that are usually on ALADINA did not work properly during DACCIWA. One explanation could be damage of optical parts after transportation, but adjusting and calibration was not possible at the research site due to missing laboratory. Thus, the current study focuses explicitly on meteorology and BC and the instrumentations are explained in the following sections."

The Vertical Variability of Black Carbon Observed in the Atmospheric Boundary Layer during DACCIWA

Barbara Altstädter[1], Konrad Deetz[2], Bernhard Vogel[2], Karmen Babić[2], Cheikh Dione[2], Federica Pacifico[3], Corinne Jambert[3], Friederike Ebus[1], Konrad Bärfuss[1], Falk Pätzold[1], Astrid Lampert[1], Bianca Adler[2], Norbert Kalthoff[2], and Fabienne Lohou[3]

[1]Institute of Flight Guidance, Technische Universität Braunschweig, Braunschweig, Germany
[2]Institute of Meteorology and Climate Research, Karlsruhe Institute of Technology, Karlsruhe, Germany
[3]Laboratoire d'Aérologie, Université de Toulouse, CNRS, UPS, Toulouse, France

Correspondence: Barbara Altstädter (b.altstaedter@tu-braunschweig.de)

Abstract. ~~The vertical variability of the~~ This study underlines the important role of transported black carbon (BC) mass concentration in the ~~atmospheric boundary layer (ABL) is analysed during the~~ West-African Monsoon (WAM) ~~season~~area. BC was measured with a micro aethalometer integrated in the payload bay of the unmanned research aircraft ALADINA (Application of Light-weight Aircraft for Detecting IN situ Aerosol)~~as~~. As part of the ~~field experiment of the~~ DACCIWA (Dynamics-Aerosol-Chemistry-Cloud Interactions in West Africa) project~~. In total~~, 53 measurement flights were ~~performed at the local airfield of~~ carried out at Savè, Benin, in ~~the period of~~ 2–16 July 2016. ~~The mean results show a~~ A high variability of BC (1.79 to 2.42 $\pm 0.31\,\mu g\,m^{-3}$) was calculated along 155 vertical profiles that were performed below cloud base in the atmospheric boundary layer (ABL). In contrast to initial expectations of primary emissions, the vertical distribution of BC was mainly influenced by the stratification of the ABL during the WAM ~~. The~~ season. The study focuses on an event (14 and 15 July 2016), which showed distinct layers of BC in the lowermost 900 m above ground level (a.g.l.). Low concentrations of NO_x and CO were sampled at Savè supersite near the aircraft measurements and suggested low impact of local sources during the case study. The lack of primary BC emission was verified by a comparison of the measured BC with the model COSMO-ART (Consortium for Small-scale Modelling–Aerosols and Reactive Trace gases) that was applied for the field campaign period~~and used in order to investigate possible sources of the measured BC. The model output was compared with the BC data on two selected measurement days (14 and 15 July 2016). The modeled~~. The modelled vertical profiles of BC ~~show that the observed~~ led to the assumption that the measured BC was already altered, as the size was mainly dominated by the accumulation mode. Further, ~~the~~ calculated vertical transects of wind speed and BC ~~showed that the measured~~ presume that the observed BC layer was transported from ~~the~~ south with maritime inflow, but was mixed vertically after to the onset of ~~the~~ a nocturnal low-level jet ~~(NLLJ)~~ at the measurement site. The ~~validations and the ground observations of gas concentrations (and) confirm that primary emission could be excluded during the case study, in contrast to initially expected. The case underlines the important role of BC transport processes~~ study contributes to the scope of DACCIWA by linking airborne BC data with ground observations and model and it illustrates the importance of a more profound understanding of the interaction between BC and the ABL in the WAM ~~area.~~ region.

1 Introduction

BC is one of the major contributors affecting the Earth's climate system. Freshly emitted BC caused by ~~the~~ incomplete combustion, is insoluble in water and it strongly absorbs the solar radiation in the visible spectrum (Bond et al., 2013). ~~However, if BC is once~~ Once BC is emitted into the atmosphere, ongoing physical and chemical reactions, like ~~the~~ secondary aerosol formation influence the composition and ~~the~~ mixing state of ~~the~~ aerosol particles. ~~BC might develop to a possible actuator~~ Aged BC can act as cloud condensation nuclei ~~(CCN), as hygroscopic growth enables coating with soluble species~~ after hygroscopic growth in the atmosphere (Zhang et al., 2008), which ultimately contributes to the indirect aerosol effect. The understanding of the BC life cycle is still poor, as ~~the monitoring of the~~ monitoring of type and source of combusted products, ~~the~~ ageing processes in the atmosphere and the current knowledge of wet deposition differ in ~~the~~ used measurement methods, and simulations show a high discrepancy (e.g., Li et al., 2017).

The role of BC emission is of ~~high~~ special interest in regions with dense population. For instance, the population in southern West Africa ~~(SWA)~~ is proposed to grow to more than 800 million by the middle of the century (Knippertz et al., 2015a), consequently a degradation of ~~the~~ air quality and ~~the~~ human health is expected by ongoing anthropogenic pollutions. Liousse et al. (2014) compared three different future scenarios for the African emissions in the year 2030, if no regulations for the combustions will be carried out. The calculated BC emission factors varied between 2 and 4 in comparison with 2005, meaning a possible emission of more than 2.5 Tg BC y^{-1} that would be comparable with 20–30 % of the BC emissions worldwide.

The impact of ~~the~~ growing air pollution on the ~~SWA~~ southern West Africa area at a regional and ~~global scale~~ global-scale is one subject of the DACCIWA project (see Knippertz et al., 2015b). ~~The project combines in-situ and aircraft observations that are further compared with satellite data and models in order to achieve a better understanding of weather, clouds and climate of SWA that is suffering from a weak monitoring network over a large area in comparison with other continental sites, e.g. in Europe and North America. The project~~ DACCIWA aims at understanding complex interactions between aerosols, clouds and their impact on ~~the~~ climate and weather in ~~SWA. The~~ South West Africa. The study combines in-situ and aircraft observations that are further compared with satellite data and models. The intensive field experiment of DACCIWA was ~~conducted~~ carried out in June–July 2016 ~~(e.g., Knippertz et al., 2017; Flamant et al., 2018; Kalthoff et al., 2018). During the study, the investigation area was affected by the occurrence of nocturnal low-level jets (NLLJ) and low-level clouds (LLC) as consequence of the WAM season (e.g., Dione et al., 2019; Kalthoff et al., 2018; Adler et al., 2019; Babić et al., 2019a). The occurrence of LLC during the monsoon are of special interest, as they affect the diurnal cycle of the ABL (Gounou et al., 2012) and their formation processes have to be integrated into models as well, as stated by Adler et al. (2017) and Hannak et al. (2017) .~~

~~The~~ during the WAM (e.g., Knippertz et al., 2017; Flamant et al., 2018; Kalthoff et al., 2018). The aerosol composition in the WAM region is mainly influenced by the large-scale synoptic pattern (Mari et al., 2008). During July and September, biomass burning smokes from southern Africa are the dominant contributors during WAM season and were proposed as a major source for BC, retrieved by satellite data and simulations (Huang et al., 2009). Horizontal transects were performed with aircraft at the coastal site of ~~SWA~~ South West Africa and the results of the PM_1 concentration were shown in Brito et al.

(2018). Interestingly, the observed BC fraction of the aerosol composition varied only minimal (6 %) above in-plume flights in comparison with ~~the background concentration~~ background concentrations of BC with 0.34 $\mu g\,m^{-3}$ in the lowermost 2 km. The observations are in agreement with ~~the simulation results~~ simulations by Huang et al. (2009), showing that BC concentration is more likely dominated by long range transport triggered by the WAM instead of local biomass burning emissions.

However, previous data showed only the ~~large scale~~ large-scale variability of BC instead of ~~local effects on smaller scales~~ columns on smaller-scales of a few square kilometres ~~at one~~ above one particular measurement field. Especially the relationship between the ABL and BC distributions needs more profound investigations. Liu et al. (2018) studied the ABL height for 347 days depending on the classification of polluted (BC $> 5\,\mu g\,m^{-3}$) and non-polluted events (BC $< 5\,\mu g\,m^{-3}$) in Wuhan, China. The ABL height was suppressed on polluted days, which ultimately leads to poorer air quality. The reduction of the ABL height can be explained by the increase of absorption due to enhanced particulate matter originating from pollution (e.g., Petäjä et al., 2016). The growing absorption heats up the upper part of the ABL which further results in an increase of stability. As cause of weaker turbulence and mixing in more stable conditions, the ABL height decreases. But in most investigations, BC is solely measured at ground. Further, Liu et al. (2018) calculated the top of the ABL from lidar measurements neglecting cases with low clouds. So that studies are missing with non-clear sky days like during monsoon seasons.

Therefore, a large benefit can be expected by using unmanned aerial systems (UAS) for investigating the ~~small scale~~ small-scale variability of BC ~~. There is a wide range of airborne platforms, including UAS operating with batteries and fuel engines, both fixed wings and multicopters that are used for observing the atmosphere with high resolution on small scales (e.g., Mayer et al., 2010; Marino et al., 2015; Renard et al., 2016; Jiménez et al., 2016; Cuxart et al., 2016; Båserud et al., 2016; Brosy et a . In order to quantify the small-scale vertical BC distribution and to understand the role of small-scale local emissions, the UAS ALADINA of aircraft type Carolo P360 (Altstädter et al., 2015) was operated during the field experiment of DACCIWA in Savè, Benin, between 2 and 16 July 2016. The ALADINA measurement period was~~ in the ABL. Relating to BC measurements, optical methods based on light-absorbing principle are common. The development of miniaturised BC instrumentation is essential, as reduced size and limitation of weight are the main challenges of new sensor integration on airborne platforms. Wilcox et al. (2016) presented vertical profiles of BC, measured with a miniaturised three wavelength absorption photometer (Corrigan et al., 2008) on UAS, during the winter monsoon over the northern Indian Ocean. BC loads were higher in the lowermost 3 km on polluted days in comparison with days of minor pollution observed at the surface. A lower ABL height was estimated during polluted days, supporting the current understanding of feedback mechanisms, like it was summarised in Petäjä et al. (2016). However, the observations showed an increase of humidity in the surface mixed layer that might favour cloud formation that is in contrast to the understanding of a lower instability and minor turbulence due to absorption of aerosols in the ABL. Thus, further studies are essential to better understand the role of BC in the ~~so-called Phase 2 lasting from the post-onset until the vortex phase of the WAM season, as stated by Knippertz et al. (2017). The first part of the period was influenced by LLC with drier periods during the vortex phase that was predominant from 9 until 17 July 2016 (Kalthoff et al., 2018). ALADINA measurements enabled the characterisation of BC mass concentrations in relation to meteorological parameters of the ABL .~~ ABL and to consider potentially other impacts on the vertical distribution in a broader range.

The objective of the current study is to investigate the ~~small scale~~ small-scale vertical variability of BC and its relation with the ABL, by using the UAS ALADINA at a remote site in West Africa~~, in general for the whole observation period, and in particular for a case study during the vortex phase with enhanced BC concentration and reduced humidity induced by long-range transport, which are unusual conditions during the monsoon period. Besides, the aim is to show the capability of an aethalometer newly implemented into the UAS.~~ . To the authors' knowledge, there is no study of the vertical distribution of BC obtained by unmanned research aircraft in the WAM region so far. ~~In addition to BC measurements, the~~ The BC distribution in the ABL is presented in general for the whole observation period (2–16 July 2016), and in particular for an event (14–15 July 2016). In order to quantify the small-scale vertical BC distribution and to assess the role of small-scale local emissions, the airborne data was compared with ground monitoring and the COSMO-ART ~~model is used in order to obtain information about the particle size and distribution . Further, the ground~~ model of the DACCIWA framework. More precisely, observations of wind profiler, ceilometer and gas concentrations are taken into account that were installed 4 km away from the research flights in order to characterise the current weather situation and possible sources for BC. The COSMO-ART model is used as indicator of particle size and distribution.

The article is structured as follows: The UAS ~~and the instrumentation integrated in the payload bay of ALADINA~~ ALADINA and its instrumentations are introduced in Sect. 2. The ~~description of the AE51 and the applied methods during post-processing are given in Subsect. 2.3. The~~ model set up of COSMO-ART is provided in Subsect. 2.4 and the measurement ~~site of the research flights and the additional ground observations at the Savè supersite~~ sites are presented in Subsect. 2.5. The results are discussed in Sect. 3 and the outcome of the study is summarised in Sect. 4.

2 Instrumentation, Model, and Measurement Site

2.1 The Unmanned Aerial System ALADINA

~~The unmanned research aircraft~~

There is a wide range of airborne platforms, including UAS operating with batteries and fuel engines, both fixed wings and multicopters that are applied for atmospheric research on a various sampling locations (e.g., Mayer et al., 2010; Marino et al., 2015; Renard . The different systems have advantages and shortcomings. In terms of ALADINA, the aircraft is electrically powered, so that any contamination of the measured air probe can be prevented. Thus, a qualitative analysis of aerosol particles is guaranteed by sampling in short periods of time, like it was done in previous studies of ALADINA (Platis et al., 2016; Altstädter et al., 2018) in Melpitz, Germany.

ALADINA was designed at the Technische Universität Braunschweig for atmospheric research and it was steadily improved regarding ~~the~~ current technical requirements~~(Fig. ??).~~ . The Carolo P360 has a maximum take off weight of 25 kg and a wing span of 3.6 m. The modular payload bay offers the capacity for a payload weight of approximately 4 kg. The pusher aircraft has an electrical propulsion and enables a flight endurance of 40–50 min at a cruising speed of 28–30 m s^{-1} in the current configuration. ALADINA is operated manually during take off and landing, whereas controlled automatically during ~~the~~ measurement flights via autopilot. ~~With the~~ Flight time, accurate position, altitude and attitude of the aircraft are given by the installed GPS (Global Positioning System) and IMU (Inertial Measurement Unit)~~the flight time, the accurate position, altitude and the attitude of the aircraft are given. Besides, a~~ . A precision of $\pm\,1.5\,\mathrm{m}$ in constant height is provided by the autopilot system. The flight track follows predefined waypoints that are sent before take off or during flight to the on board computer and can be changed according to the current scientific goals during ~~the~~ measurement flights. ~~The data and the~~ Observed data and flight path can be monitored via live transfer at a temporal resolution of 1 Hz.

More information on the airplane itself can be found in Altstädter et al. (2015)~~, and an update of the current instrumentation~~ . The instrumentation was updated for DACCIWA and the set up is provided in Bärfuss et al. (2018). ~~Further, the~~ All UAS data derived during DACCIWA ~~can be taken from Bärfuss et al. (2017)and more information on the meteorological data of the UAS is available in ?. The meteorological sensor package is displayed in Fig. 1a and~~ are available from Bärfuss et al. (2017) . Other aerosol sensors (optical particle counter and condensation particle counter) that are usually on ALADINA did not work properly during DACCIWA. One explanation could be damage of optical parts after transportation, but adjusting and calibration was not possible at the research site due to missing laboratory. Thus, the ~~micro aethalometer is shown in Fig. 1b. The measuring devices used in the~~ current study focuses explicitly on meteorology and BC and the instrumentations are explained in the following sections.

2.2 Meteorological Sensors for Turbulence Measurements

The meteorological ~~sensors are mounted at the tip of the aircraft nose in order to assure an undisturbed air flow. Figure 1displays the~~ sensor package is displayed in Fig. 1a. It consists of a multi hole probe (number 1), ~~the~~ temperature sensors (number 2–4) and ~~the~~ humidity sensors (number 4 and 5). The meteorological sensors are mounted at the tip of the aircraft nose in order to assure an undisturbed air flow.

The three dimensional wind vector ($\boldsymbol{V}$) is derived via a multi hole probe manufactured by the Institute of Fluid Dynamics (Technische Universität Braunschweig, Germany; e.g., Wildmann et al., 2014). The multi hole probe is combined with an IMU/GPS system. The wind vector has a usable data rate of up to 100 Hz with an accuracy in ~~the~~ wind speed components of $\pm\,0.5\,\mathrm{m\,s^{-1}}$ and in ~~the~~ wind direction of $\pm\,10\,°$. The methods for ~~the~~ wind calculation are described in Bärfuss et al. (2018). ~~Figure ??a shows the power spectra of the wind vector components u, v and w during a horizontal flight in the altitude of 100 m a.s.l. on 2 July 2016. The signal power was compared with the Kolmogorov law for isotropic turbulence (green dotted line) and indicates that the spectral behaviour is in agreement with the expected distribution of up to a frequency of 10 Hz.~~

The air temperature is calculated from three temperature sensors based on different measurement techniques. A finewire element was manufactured at the Institute of Flight Guidance with a high temporal resolution of 30 Hz and an accuracy better than $\pm\,0.05\,\mathrm{K}$ (see Fig. 1a, number 2). The sensor principle is comparable with a system described in Wildmann et al. (2013), but it was additionally protected with a housing against direct solar radiation, dust particles and mosquitoes. In addition, a factory calibrated capacitive sensor of type TSYS01 (Measurement Specialties, USA) was used with a resolution of around 0.3 Hz and a given accuracy of $\pm\,0.1\,\mathrm{K}$ (see Fig. 1a, number 3). These two sensors were fused together into a long term stable reading with an error of less than $\pm\,0.1\,\mathrm{K}$ and used for this study. Further, the air temperature was measured by an HMP110 (Vaisala, Finland) with lower resolution of 0.5 Hz and $\pm\,0.2\,\mathrm{K}$ accuracy (Fig. 1a, number 4). ~~Figure ??b represents the power~~

~~spectra of the potential temperature θ after post-processing for the same horizontal flight on 2 July 2016. The signal power follows the Kolomogrov law up to the frequency of 9 Hz.~~

The relative humidity is measured with a Rapid P14 Element (Innovative Sensor Technology, Switzerland) and a HMP110 (Vaisala, Finland), both based on ~~the~~ capacitive measuring principle (Fig. 1a, number 4 and 5). The measurement range is from 0 to 95 % RH with an accuracy of ± 1.5 % RH in a temperature range between 0 and 40 °C specified by the manufacturer. The response time of 10 s resulted after combining the humidity sensors complementary.

2.3 Aethalometer for Detecting ~~the~~ BC Mass Concentration

The one wavelength micro aethalometer (microAeth® model AE51, AethLabs, USA) is a ~~lightweight tool for monitoring the BC mass concentration~~light weight (around 280 g) and easy handling device for BC monitoring. It was implemented into the payload bay of ALADINA (see Fig. 1b). The aerosol inlet is installed at the front of the aircraft close to ~~the~~ meteorological sensors (Fig. 1a, number 6). The air stream was run at a flow rate of 150 ml min^{-1} and it was dried with silica gel before reaching the AE51 inlet in order to avoid strong influences of moisture on the filter stripe of the sensor. ~~The measurement range is 0–1 mg~~

Here, it has to be considered that different measurement methods (for instance optical or chemical) lead to different types of BC ~~m^{-3} with a resolution of 1 ng BC m^{-3} specified by the manufacturer. After testing the micro aethalometer in the laboratory and in the field, the accuracy was determined to ± 0.2 µg BC m^{-3} at a response time of 1 Hz. The effects of meteorological conditions (sensitivity to temperature and humidity changes) on the instrument's readings and artefacts were characterised on different types of airborne platforms (e.g., Ferrero et al., 2014; Ran et al., 2016; Chiliński et al., 2018) and will be further validated with the observations.~~. A clear terminology is mandatory, as recommended by Petzold et al. (2013). In terms of the presented study, the equivalent black carbon (EBC) was calculated from the AE51. Only for the sake of simplicity, the term BC instead of EBC will be used hereafter.

The BC mass concentration is estimated from the attenuation coefficient (σ_{ATN}) at the wavelength of 880 nm on an aerosol loaded filter. In case of ~~the~~ AE51, a T60 Teflon-coated borosilicate glass fibre filter stripe is used that has to be manually changed after every measurement period. The measurement principle is based on the Lambert-Beer law and the attenuation (ATN) is defined as follows:

$$ATN = -100 \cdot ln\left(\frac{I}{I_0}\right), \tag{1}$$

where the attenuation is calculated from the ratio of the light intensity (I) transmitted through the loaded filter in comparison with the initial intensity of the transmitted light (I_0) on an aerosol-free filter stripe. Taken from Hansen et al. (1984), the attenuation is proportional to the surface concentration of BC. Taking into account that the change in the attenuation (ΔATN)

is caused by an increasing BC mass load on the filter stripe in a corresponding time interval (Δt), the BC mass concentration can be derived as follows (Saturno et al., 2017):

$$BC = \frac{\sigma_{ATN}}{\alpha_{ATN}} = \frac{A \cdot \Delta ATN}{\alpha_{ATN} \cdot Q \cdot \Delta t}. \tag{2}$$

A is the filter stripe area, α_{ATN} is the BC mass attenuation cross section at the wavelength of 880 nm and Q is the volumetric flow rate.

σ_{ATN} was corrected due to artefacts based on the filter-based measurement technique (e.g., Weingartner et al., 2003; Virkkula et al., 2007; Collaud Coen et al., 2010; Ran et al., 2016). ~~In addition, the micro aethalometer is~~

The measurement range is 0–1 mg BC m^{-3} with a resolution of 1 ng BC m^{-3}, specified by the manufacturer. After testing the micro aethalometer in the field and in the laboratory afterwards, the accuracy was determined to $\pm$ 0.2 µg BC m^{-3} at a response time of 1 Hz.

The effects of meteorological conditions (sensitivity to temperature and humidity) on the instrument's readings and artefacts were characterised on different types of airborne platforms (e.g., Ferrero et al., 2014; Ran et al., 2016; Chiliński et al., 2018). However, a direct comparison of the AE51 on UAS relating to ground observations was missing so far. Pikridas et al. (2019) showed that the AE51 is a feasible tool for BC measurements on UAS in an area of high background aerosol particle concentration. Flight campaigns were conducted in Athens and Cyprus. The results are based on comparison of three different miniaturised absorption instruments (e.g. AE51) on UAS with ground based monitoring of MAAP (Multi Angle Absorption Photometer) and one micro aethalometer of type AE33. According to results of the Athens campaign, the correlation of AE51 was R^2=0.76 by sampling close to ground in relationship between MAAP and AE33. BC was underestimated by the AE51 of 6 to 7%, thus within the given accuracy of 10%. However, the comparison during the Cyprus campaign showed a high overestimation of 22–55% BC by the AE51, possibly caused by low background aerosol particle concentration at the research site. The low performance of the instrument for small background concentration in generally clean air masses is one major issue of the AE51 (e.g., Ferrero et al., 2014; Lee, 2019). The impact should be of minor relevance for the current study that addresses an area with high PM concentration, partially higher than WHO guidelines (Adon et al., 2019). However, during laboratory tests it became apparent that readings of the micro aethalometer are also sensitive to changes in temperature and humidity~~as described in the following section.~~. This will be further addressed.

2.3.1 Influence of Temperature Changes and Data Post-Processing

As example, the impact of ~~the~~ temperature changes on the attenuation is shown for a flight that was performed with ALADINA on 14 July 2016 (flight ID 41 of ~~the~~ 53 total measurement flights). Figure 2 presents the internal temperature from the micro aethalometer (PCBtemp) during the measurement period from 05:16 until 06:30 UTC that varied between 27 and 36 °C. This flight was chosen as the worst case scenario during the study. In order to determine the temporal evolution of ~~the~~ temperature, the bit noise has to be filtered out by any smoothing algorithm. ~~In the laboratory tests~~ Taken from laboratory tests in a temperature chamber, the influence factor of temperature changes on ~~the~~ BC measurements was determined to be in the order of 0.25 µg BC $(dT/dt)^{-1}$. Applied for the current case, ~~the~~ largest temperature gradients were observed between 05:16 and 05:30 UTC during the first steps of the ascent, leading to a bias (shown in BC Error, lower panel of Fig. 2) of 3 µg BC m^{-3}. ~~For the whole study, the~~ BC data were corrected with the internal temperature changes measured directly at the BC sensor ~~.~~ for the whole study. Here, it should be clarified that these first steps of ascent, and similar to all other flights, do not directly affect the here presented analysis. These first steps correspond to take-off that is handled in remote control by the responsible pilot. However, exclusively automatic flight tracks were used in order to obtain comparable vertical profiles and neglecting horizontal patterns. One possible cause of these large temperature gradients might be internal heating of the aircraft. During landing and preparation of the next research flight, the aircraft was exposed directly to sunlight. Another effect that could lead to this high BC error, might be the load of the optical part. The error was reproducible in the laboratory, but the exact source of the error could not be determined. More tests in field studies would be mandatory.

During post-processing, the readings of the BC attenuation were phase shift free low pass filtered at different time scales in 10, 30 and 60 seconds. ~~Figure 3~~ Therefore, a high pass Butterworth filter of third order was used, running forward and backward in order to eliminate phase shifts. Averaging was not applied for the attenuation signal in avoidance of poor frequency responses. Figure 4 shows the high ~~variance~~ variability of the attenuation signal for 1 s temporal resolution during a measurement flight between 15:58 and 16:42 UTC on 10 July 2016. The results with the highest possible temporal resolution but still acceptable noise (standard deviation smaller than 0.3 µg m^{-3} or 22% of the signal) were obtained by a low pass filter with a span of 10 s. ~~This method was further used for the study.~~ The mean attenuation ~~after 10 s low pass filtering~~ was 1.59 ± 0.30 µg m^{-3}, varying between 0.5 and 2.5 µg m^{-3}. As the frequency response will be lost by a span of 30 s or more, the method of 10 s low pass filter was used for BC measurements of ALADINA profiles, except for the model comparison in Sect.3.3. The simulations were run prior to statistic overview in Sect. 3.1 with a span of 1 s.

2.4 Model Description of COSMO-ART for DACCIWA

In this section, a short description of the model COSMO-ART (Consortium for Small-scale Modelling–Aerosols and Reactive Trace gases) and the simulation set up for the DACCIWA measurement campaign are shown. COSMO-ART is a comprehensive online coupled model system (Vogel et al., 2009) based on the operational weather forecast model COSMO (Baldauf et al., 2011). COSMO-ART includes a comprehensive chemistry module to describe the gaseous composition of the atmosphere and secondary aerosol formation. Chemical reactions are calculated with RADMKA (Regional Acid Deposition Model Version Karlsruhe; Vogel et al., 2009), which is based on RADM2 (Regional Acid Deposition Model, Stockwell et al., 1990). Physical processes, including transport, turbulent diffusion, and dry and wet deposition are treated together with photochemistry and aerosol dynamics using the modal approach. The size distribution of aerosol within COSMO-ART is approximated by eleven log-normal distributions (modes), considering the Aitken and nucleation mode (with and without BC core), fresh BC, and the coarse mode (sea salt and mineral dust). COSMO-ART explicitly treats the ageing of BC particles transferring them from external to internal mixtures as described in Riemer et al. (2004). For DACCIWA, the COSMO-ART model system was applied quasi-operational during the DACCIWA measurement campaign, to support the decision-making of research aircraft flight tracks within the aircraft special observing period (27 June–17 July 2016) and to derive model climatologies of the spatial distribution of the southern West African air pollution. More details of the model set up for DACCIWA can be taken from Deetz et al. (2018). The continuous forecasts were initiated on 8 May and were active until 31 July 2016, covering the simulation domain 25 °W–40 °E and 20 °S–35 °N with a grid mesh size of 28 km and 3 h model output. ICON forecasts were used as meteorological boundary conditions and MOZART (Model for OZone and Related chemical Tracers) as aerosol/chemistry boundaries. The simulations consider the emission of mineral dust, sea salt, biogenic volatile organic compounds, dimethyl sulphide and emissions from biomass burning and anthropogenic origin. BC is related to the anthropogenic emissions and the emissions from biomass burning. The feedbacks of the prognostic aerosol on the aerosol direct and indirect effect are not considered in these simulations.

2.5 Measurement Site

The measurement flights were performed at the local airfield (8 °1′N, 2 °27′E, 185 m above sea level, a.s.l.) south-west of Savè, Benin, in the period between 2 and 16 July 2016. The commune covers an area of 2×10^4 km^2 with approximately 100,000 inhabitants. The Savè supersite of Karlsruhe Institute of Technology (KIT) and Université de Tolouse (Université de Toulouse III- Paul Sabatier, UPS) was installed at a distance of 4 km SW of the airfield close to Gobè (Fig. 4). An overview of the Savè supersite and ~~the~~ mounted instrumentation are given in Kalthoff et al. (2018). Both measurement sites are connected with the main road RNIE2. The airfield consists of dry and sandy soils and is surrounded by agricultural land. During the experiment, 53 flights were performed on different daytimes with a total flight duration of 32 h and a total flight distance of approximately 2260 km. Within the study, 155 vertical profiles were realised up to a maximum height of 1600 m a.g.l. allowing the analysis of ABL conditions in connection with the vertical distribution of BC. Although ~~the~~ Savè supersite was at a distance of 4 km, horizontal flights were in most cases directed parallel to the current wind direction measured at the supersite.

A typical flight pattern of a horizontal leg can be seen in Fig. 5. The black dashed line shows the flight track of one measurement flight on 14 July 2016. The starting point of the UAS is marked with the black dot at the latitude of 8.0171 °N and the longitude of 2.4637 °E. Further, the wind speed is shown along four selected horizontal legs at the height of 520 m a.s.l. The wind speed varied between 7 and 11 m s^{-1} (blue to red in the colour bar) and shows a dependence on the horizontal scale, as the wind speed increased in the south and in the direction of the Savè supersite.

2.5.1 Ceilometer and Wind Profiler

In order to retrieve information on cloud cover, cloud base height~~(CBH)~~, wind speed and wind direction during the UAS operation, ceilometer and wind profiler data were used from the Savè supersite.

The CHM15k ceilometer was employed to obtain the temporal evolution of cloud characteristics during the DACCIWA campaign (Handwerker et al., 2016). From the measurements of the attenuated backscatter coefficient profiles the ~~CBH~~ cloud base height is determined based on a threshold method (manufacturer Lufft, personal communication, 2016). The manufacturer algorithm allows for the detection of up to three ~~CBHs~~ cloud base heights at a temporal resolution of 1 min and 15 m vertical resolution. In this study, only the first detected ~~CBH~~ cloud base height is shown, since the focus is on ~~the LLC~~low-level clouds.

High-resolution information of flow conditions (wind speed and wind direction) is obtained from a sodar (for the lower part of the ABL, Wieser et al., 2016) and an ultra-high-frequency (UHF) wind profiler (above 200 m a.g.l.) measurements.

The sodar is an active remote sensing instrument, which was continuously running during the campaign. The retrieved information is based on the reflection of acoustic pulses at temperature inhomogeneities in the air with subsequent Doppler analysis. The instrument provides profiles of horizontal wind speed and direction and the backscatter at ~~the~~ 30 min temporal resolution and 10 m vertical resolution between 30 and 600 m a.g.l. in altitude.

The UHF wind profiler installed at Savè supersite by UPS is a 1274 MHz Doppler radar and it works with five beams to document the vertical structure of ~~the~~ atmospheric dynamics up to the middle troposphere. It allows the retrieval of the three components of the wind. The wind profiler operated continuously from 19 June to 30 July 2016 with two acquisition modes (75 and 150 m vertical resolution, respectively) in a time resolution of ~~two minutes~~2 min. This radar is used in Dione et al. (2019) for the characterisation of the low-level atmosphere dynamics during the whole DACCIWA campaign. More details on the data availability and the technical characteristics of this radar can be found in Derrien et al. (2016). In this study, the data was averaged over 15~~minutes~~ min using the low mode (0-3 km) for the analysis of the wind speed and direction during the studied days.

2.5.2 Gas Concentrations of NO_x and CO

Measurements of trace gases were taken on two separate towers. Nitrogen monoxide (NO) and nitrogen dioxide (NO_2) were measured on an 8 m high tower and carbon monoxide (CO) was measured separately at 3.50 m above ground level (a.g.l.). Both towers were located at the Savè supersite, 80 m away from each other, and were generally upwind from the main neighbouring town of Savè and the power generator used for the whole instrumentation.

CO atmospheric mixing ratios were measured with a modified Model 48C-TL CO Analyzer (Thermo-environmental Instruments Inc.) with a detection limit of 12 ppb_v. A dynamic dilution method by flow regulators is used for the CO calibration. The dilution is made with a commercial reference CO-N2 mix at 450 ppm_v (air liquid bottle) into zero air made by Sofnocat 423. Every 3 or 4 years, the flow regulators device is send to French Laboratoire national d'Essais for check and calibration.

NO and NO_2 were measured with a Model 42C-TL NO-NO_2-NO_x (Thermo-environmental Instruments Inc.) with 0.05 ppb_v detection limit. The Model 42C-TL NO-NO_2-NO_x was calibrated before and after the campaign by using a reference NO_2 air mixture, i.e. NO in N_2 diluted with zero air. Reference NO, and NO_2 were ISO 6141:2015 certified at 8.73 and 8.58 ppm for NO, before and after the campaign, respectively, and 9.28 ppm for NO_2, both with 5 % precision (Pacifico et al., 2019).

All data of the trace gases were sampled every 10 ~~seconds~~s, filtered and averaged to produce 1 and 30 ~~minutes~~ min values. The data is accessible from Derrien et al. (2016).

3 Results and Discussion

~~In this study~~First, an overview of the small-scale vertical variability of BC is presented from measurements of ALADINA during the two week ~~measurement period of the DACCIWAfield experiment is presented~~period (2-16 July 2016) of DACCIWA.

For this, the vertical distribution of the observed BC mass concentration is shown in relation to the structure of the ABL based on 155 vertical profiles~~obtained with ALADINA~~. Further, a particular case ~~with the typical WAM conditions lasting from 14 until 15~~ (14-15 July 2016~~is analysed that emphasizes the dependence of BC concentration on transport processes. Simulation results of COSMO-ART are compared to the BC profiles obtained by ALADINA to achieve a better knowledge of the contributors and the possible sources of the observed BC.~~) with enhanced layer of BC is analysed in detail.

3.1 Summary of the Vertical Variability of BC during the Experiment

Figure 6a shows ~~the~~ BC mass concentration, ~~the~~ potential temperature and ~~the~~ water vapour mixing ratio calculated in 20 m intervals in the lowermost 1100 m a.g.l. along 155 vertical profiles. Figure 6b represents the standard deviation of the mean profiles for corresponding parameters shown in Fig. 6a. The vertical distribution of the minimum BC mass concentration was almost not detectable in the lowermost 600 m a.g.l., but increased up to $1.64 \pm 0.2\,\mu\text{g}\,\text{m}^{-3}$ at higher altitudes. The total maximum of $14.01\,\mu\text{g}\,\text{m}^{-3}$ was measured ~~in~~ at the height of 200 m a.g.l., but was only observed during one day on 15 July 2016. The mean BC mass concentration ($\overline{BC}$) varied between $1.79\,\mu\text{g}\,\text{m}^{-3}$ and $2.42\,\mu\text{g}\,\text{m}^{-3}$, and the standard deviation for all altitude intervals was $\pm\,0.31\,\mu\text{g}\,\text{m}^{-3}$. The vertical distribution of $\overline{BC}$ showed three dominant distinguished layers at the heights of 200, 600 and 920 m a.g.l. (Fig. 6b). The mean potential temperature ($\overline{\theta}$) was between 300.6 and 304.1 K in the vertical distribution and represented an overall stable stratification of the ABL, as the majority of the measurement flights was performed in the morning hours. The mean water vapour mixing ratio ($\overline{q}$) varied between 14.24 and $16.24 \pm 0.52\,\text{g}\,\text{kg}^{-1}$ and decreased with altitude in the lowermost 1100 m a.g.l.

All mean values showed a sharp gradient at the height of 600 m a.g.l. One explanation for this could be less data availability above this height. The research flights are restricted below cloud base, as ALADINA is not rain proof. The first part of the measurement period (2-8 July 2016) was during the post-onset phase of the WAM season (Knippertz et al., 2017). This period was influenced by low-level clouds with a median height of cloud top at 587 m a.g.l., taken from 06:00 UTC radiosondes at Savè (Kalthoff et al., 2018). This part corresponds to almost half (25 of 53) of the research flights. Although, nocturnal low-level clouds dissolved during the day, a large portion of vertical profiles still remained below 600 m a.g.l. Drier periods occurred during the vortex phase of the WAM that was predominant from 9 until 17 July 2016 (Knippertz et al., 2017).

Taken from the statistic overview of $\overline{BC}$, BC seems to occur in the whole ABL. No clear evidence is visible of local pollution near surface. One explanation could be the performance of ALADINA during daytime so that in some cases the ABL was already well mixed and BC was lifted from ground through the ABL. However, this can not be supported by $\overline{\theta}$ that shows an overall stable ABL. This relationship presumes that observed BC originated prior to the observation periods, probably during night or even earlier. Another possibility could be horizontal advection that caused distinguish layers of BC in the ABL. Here, the understanding of BC in the ABL can not be fully described by previous observations like Wilcox et al. (2016) and Liu et al. (2018). Directly emitted BC would have probably warmed the ABL by absorption that further caused stable conditions and a lower ABL height but with increased humidity. This is in contrast to here observed reduced humidity due to the decline of $\overline{q}$ in the ABL. Therefore, it is essential to take into account other aspects that might affect the BC distribution within the ABL.

3.2 BC Observations during Case Study on 14–15 July 2016

The following section addresses the vertical distribution of BC measured with ALADINA on two days in this period (14 and 15 July 2016)~~that were influenced by the NLLJ~~. The first day was influenced by a nocturnal low-level jet and free of ~~LLC (14 July 2016), which is related to the vortex phase, and influenced by the NLLJ and LLC (15 July 2016)~~low-level clouds. The second day was affected by a nocturnal low-level jet and by the presence of low-level clouds, see Babić et al. (2019b).

An overview of the performed measurements ~~during the case study~~ is presented in Tab. 1. The flight time of ALADINA is given in UTC (local time = UTC +01:00). In addition, ~~the 1 min averaged~~ gas concentrations of NO_x and CO (Derrien et al., 2016) are presented for the flight periods in 1 min average. The total maximum NO_x concentration of 1.9 ppb$_v$ was observed in the morning between 06:41 and 08:40 UTC on 15 July 2016 simultaneously with the maximum CO concentration of 259 ppb$_v$~~of the concentration.~~.

Backscatter data indicate that there ~~is~~ was a well mixed layer in the afternoon ~~of~~ on 14 July 2016, and ~~LLC~~ low-level clouds appeared temporarily above 800 m a.g.l. (Fig. 7a). On the following day, ~~LLCs~~ low-level clouds formed below 250 m a.g.l. at about ~~7~~ 07:00 UTC (Fig. 7b).

The enhanced aerosol load disappeared, which can be seen by the enhanced backscatter at an altitude up to 300 m a.g.l. from midnight to ~~7~~ 07:00 UTC in Fig. 7b. Afterwards, the clouds lifted up to 750 m a.g.l. at 11:00 UTC and dissolved completely at 14:00 UTC in the lowermost 2 km a.g.l. In addition, a second layer of clouds built up at the height between 1050 and 2000 m a.g.l.

Wind conditions are shown in Fig. 8. The wind speed was moderate between 3 and 6 m s^{-1} in the lowermost 2 km a.g.l. in the night from 13 July until the early morning at 06:00 UTC on 14 July (Fig. 8a). The observed ~~LLJ~~ low-level jet intensified in the course of the night and reached the maximum speed in the early morning hours. The strip of high wind speed has dissolved at midday, simultaneously with the occurrence of clouds. However, in the afternoon, there is a low-level wind maximum of 6–8 m s^{-1} at the height between 200 and 600 m a.g.l. that persisted for more than 12 h at the same altitude (Fig. 8b). At 07:00 UTC on 15 July, when ~~LLC~~ low-level clouds were present, the wind speed reached a maximum of 9 m s^{-1} between the height of 800 and 1000 m a.g.l. After the dissolving cloudiness at 12:00 UTC, a wind speed of 3 m s^{-1} was observed. ~~Wind~~ Measured wind speed and wind direction are a combination of the persistent monsoon flow and the maritime inflow that arrives typically in the early evening hours ~~Dione et al. (2019); Adler et al. (2019)~~(Dione et al., 2019; Adler et al., 2019).

Figure 9a displays three vertical profiles between the height of 100 and 800 m a.g.l. obtained with ALADINA at 06:15, 06:55 and 07:27 UTC on 14 July 2016. The ABL was stably stratified with the base of the inversion layer at 400 m a.g.l. At the heights of 450 to 500 m a.g.l. a dry air mass was observed, as can be seen from the profile of the water vapour mixing ratio. Above the inversion layer and in accordance with the different type of air mass, an increase of BC was observed in the residual layer~~(RL)~~. The total maximum BC of 2.75 µg m^{-3} was ~~observed~~ measured at the height of 600 m a.g.l. in the first profile at 06:15 UTC~~, and the~~. The enhanced BC concentration at this altitude was still visible 1 h later. The wind direction varied between SE and SW and the vertical distribution of the wind speed showed a significant increase close to the inversion layer. At 07:27 UTC the wind speed increased up to 12 m s^{-1} between the height of 400 and 500 m a.g.l.

The structure of the ABL was ~~well-mixed~~ well mixed at noon and before the evening transition (Fig. 9b) leading to homogeneous conditions of q and BC in the vertical distribution. The wind direction changed from SW to SE in the lowermost 200 m a.g.l. and the wind speed was constant with 5 m s^{-1} in the lowermost 800 m a.g.l.

On the following day (15 July 2016) the ABL was influenced by the formation of ~~LLC~~ low-level clouds around 07:00 UTC. The same parameters as shown in the previous part are presented in Fig. 10. In this case, three vertical profiles are displayed at 05:33, 06:10 and 06:46 UTC before ~~the LLC~~ low-level clouds occurred. The UAS was operated between 100 and 900 m a.g.l. and the ABL was stable with a capping inversion layer ~~between 300 and 400~~at 300–400 m a.g.l. The fourth vertical profiles was performed at 08:29 UTC below the cloud base maximum height of 320 m a.g.l. The last profile was carried out at 16:52 UTC after the dissolution of ~~LLC~~ low-level clouds below 650 m a.g.l. The ABL was ~~well-mixed~~ well mixed and q decreased in comparison with the profiles in the morning hours. ~~The impact of the LLC on the BC mass concentration can be clearly seen in the decline of BC with a difference of~~ BC decreased to 1.5 µg m^{-3} at the height of 300 m a.g.l. One explanation could be wash out by low-level clouds. An other ~~impact of the vertical variability~~ possibility of BC reduction might be caused by the change in ~~the~~ wind direction to SSW~~during the day, so that~~. Probably, a different type of air mass ~~was observed~~with cleaner air was observed in the investigating area. The wind speed increased close to ground level up to 5 m s^{-1} but decreased to 3.2 m s^{-1} at 600 m a.g.l.

3.3 Comparison of ALADINA Observations with COSMO-ART Model Results

In this section, ~~the~~ ALADINA BC profiles are compared with the model results of COSMO-ART obtained during the case study. For the comparison it has to be considered that COSMO-ART has a grid mesh size of 28 km and the lowest 1000 m are resolved by only eleven layers. This makes a direct comparison with ~~the~~ airborne point observations difficult. Nevertheless, the simulations with COSMO-ART provide added value to this study: ~~On the one hand,~~ BC can be separated into fresh BC, aged BC in the Aitken and aged BC in the accumulation mode, allowing to discuss potential sources of BC. ~~On the other hand, the~~ Further, simulations allow to embed the local observations into larger spatial scales. Riemer et al. (2004) indicated BC ageing time scales of 8 h close to ~~the~~ source regions and 2 h above ~~the~~ source regions for daytime conditions during summer, predominantly related to ~~the~~ ageing via the condensation of sulphuric acid on BC particles.

Figure 11 shows the spatio-temporally collocated total BC profiles of ALADINA with 1 Hz temporal resolution and COSMO-ART for six different time intervals. In addition, the COSMO-ART results for fresh BC, aged BC (Aitken mode) and aged BC (accumulation mode) are indicated.

For 14 July 2016 (see Fig. 11a–d) a full diurnal cycle of BC profiles from 06:00 to 18:00 UTC is presented. In the morning hours the observations show increased concentrations above 500 m a.g.l. with the peak of around 3.0 µg m^{-3} at 600 m a.g.l. (Fig. 11a). This peak is ~~well captured by~~ represented in the model. The best agreement is found for aged BC in the accumulation mode. However, COSMO-ART shows near-surface concentrations of up to 3 µg m^{-3} that are higher than the observations. Until noon, the vertical profile of BC shows a vertically constant BC concentration, likely due to ~~the~~ vertical mixing in the ABL (Fig. 11b and c). COSMO-ART results of aged BC in the accumulation mode match very well these observations. The observed BC concentration peak at the altitude of 900 m a.g.l. is not seen by COSMO-ART, and may be an artifact induced by the formation of cloud patches as seen by the ceilometer (Fig. 7a). Between 12:00 and 18:00 UTC, no significant change in the measured vertical BC profile is visible. In the simulations, the contribution of BC in the accumulation mode decreases and the concentration of BC in the Aitken mode increases, leading to a better agreement of the observations with the total BC concentration (Fig.11d). At 06:00 UTC on 15 July 2016 (see Fig.11e) observation and model indicate an enhanced BC concentration below 400 m~~.~~ a.g.l. The vertical profile, capturing the lowest 900 m~~, agrees very well between~~ a.g.l., shows a representative agreement of observation and model of ~~the~~ total BC. Around the height of 200 m a.g.l., ALADINA indicates ~~very~~ high BC concentrations of more than 16 $\mu g\,m^{-3}$ that are not represented in COSMO-ART. ~~It~~ The discrepancy could be based on the 1 s sampling of ALADINA that is strongly noisy. The first assumption was turbulent mixing near the cloud edge that might have led to high variability of the sampling flow, thus on BC data. Another possibility could be droplets that disturbed the signal. However, it cannot be ruled out that this is an artifact induced by ~~the~~ high humidity prior to the onset of cloud formation, which occurred around that time. Finally, at 18:00 UTC, the observed BC profile ~~agrees well with~~ corresponds to the aged BC in the accumulation mode.

Figure 12 shows a South-North cross section of the total BC concentration and wind speed up to an altitude of 1500 m a.g.l. for 14 July 2016. The location of the airborne observations at Savè is indicated by the dashed line. The wind speed transect clearly shows the ~~NLLJ~~ nocturnal low-level jet with its maximum around the height of 500 m a.g.l.. From 13 July 2016 at 21:00 UTC until 14 July 2016 at 09:00 UTC, the jet propagates northwards. The vertical transect of the BC concentration indicates that the ~~LLJ~~ low-level jet is linked to lower BC concentrations, which ~~is confirmed by the ALADINA observations between~~ was observed with ALADINA at 06:15 and 07:30 UTC on 14 July 2016 (Fig. 9), as well. The coastline is approximately at 6.2 °N, so the low BC concentrations especially occur over the Gulf of Guinea. In front of the jet, an air mass with high BC burden (up to 20 $\mu g\,m^{-3}$ near the surface) is visible. At 00:00 UTC, the BC concentration maximum is directly over Savè, however, this is not related to local emissions. ~~Four~~

Three aspects seem to justify this hypothesis: (1) ~~The transects east and west of the shown Savè transect provide a similar pattern (not shown). Therefore it is rather a zonal symmetrical feature than a local Savè feature~~Concentrations of NO_x and CO do not indicate anthropogenic local emissions for the observed time period. (2) Fig. 11 shows negligible fractions of fresh BC which indicates less influence of local emissions. (3) ~~Concentrations of and CO (not shown) do not indicate anthropogenic local emissions for the observed time period. (4)~~ By considering also the time steps before 13 July 2016 at 21:00 UTC, it becomes clear that the polluted air mass is transported from the South in front of the northward propagating maritime inflow. Since the ~~LLJ~~ low-level jet has its maximum around 500 m in altitude, the clean air mass of the jet puts a wedge into the polluted air mass in front (e.g. visible on 14 July 2016 at 06:00 UTC). This leads to a near surface pollution branch below the jet axis and an elevated pollution branch above the jet axis. This is also visible in the modelled profiles of Fig. 11a, and in the observed profiles, a clearly enhanced BC concentration in the upper branch, a minimum at around 400-500 m a.g.l. and a slightly enhanced near-surface BC concentration is visible. At 12:00 UTC, the vertical mixing in the ~~boundary layer~~ ABL leads to a rather homogeneous distribution of BC in the vertical profile. Even if the peak observed at 12:00 UTC around 900 m a.g.l. over Savè (see Fig. 11c) may be partly induced by cloud artifacts, its altitude fits to the location of the modelled elevated pollution branch in Fig. 12. From 14 July 2016 at 12:00 UTC on, a reestablishment of a pollution layer can be observed between 7 °N and 8 °N.

4 Conclusions

This ~~study focused on the~~ article aims at understanding the relationship between the vertical distribution of BC in the ABL ~~obtained with the unmanned aerial system ALADINA, that was operated during the~~ in southern West-Africa. The investigation area is supposed to be one of the major sources for BC emissions worldwide (Liousse et al., 2014). But where do those BC emissions originate, especially in the ABL? Beyond surface measurements, the role of BC is difficult to assess within the ABL due to lacking column measurements. ALADINA was applied for meteorological profiling and BC measurements during the extensive field experiment of DACCIWA ~~between 2 and 16~~ at Savè, Benin, in 2–16 July 2016. ~~In total, 53 measurement flights were carried out up to a maximum height of 1600 m a.g.l. at the local airfield of Savè/Beninin West Africa.~~

BC was measured with a micro aethalometer, model AE51, ~~on board the new set up of ALADINA (Bärfuss et al., 2018). After low pass filtering the attenuation coefficient~~ that has been proved as feasible tool on UAS, but it suffers from artefacts that were one subject of this paper. Prior to analyses, BC data were corrected with bias caused by the dependence of the instrumentation on internal temperature during ascents and descents. Further, a low pass filter was applied for the readings with a resolution of 10 s.

For a statistical overview, BC was averaged for altitude intervals of 20 m steps along 155 vertical profiles ~~for a statistical overview. In addition, the BC data was further corrected with bias caused by the depenence of the instrumentation on internal temperature during ascents and descents.~~ of the whole measurement period. In contrast to initially expectations, no clear influence of primary BC emission was observed in the vertical distribution. It was shown that BC occurred in the whole ABL and did not decrease depending on the altitude. Thus, maxima and minima of BC concentration ~~are related~~ could be caused by other aspects than solely from ABL conditions. One explanation could relate to horizontal advection processes ~~, and not local emissions.~~ that might have brought about different types of air masses with distinguished layers of BC. Another explanation could be based on regional-scale. The measurement period was influenced by the WAM season, leading to high occurrence of nocturnal low-level jet and low-level clouds that could have strongly affected the vertical distribution of BC due to dynamics in the ABL. (e.g., Dione et al., 2019; Kalthoff et al., 2018; Adler et al., 2019; Babić et al., 2019a).

One case study (14–15 July 2016) was presented in detail ~~, influenced by NLLJ and LLC-free on 14 July, and influenced by NLLJ and LLC on 15 July 2016.~~

~~A~~ in order to clarify possible other impacts on the BC distribution. Therefore, ground observations of wind profiler, ceilometer and gas concentrations were used from Savè supersite, 4 km away from the research flights. NO_x and CO did not show any clear evidence of local emissions at ground. However, a maximum of BC=$2.81 \pm 0.30\,\mu g\,m^{-3}$ was observed in the ~~RL~~ residual layer between the heights of 400 and 600 m a.g.l. in relation to ~~the NLLJ~~ a nocturnal low-level jet with wind speeds larger than $12\,m\,s^{-1}$. The lifted BC layer was vertically mixed during clear sky conditions during the day and the mass concentration increased continuously in the lowermost 1100 m a.g.l. On the next day, ~~LLC~~ low-level clouds formed in the early morning that might have led to wash out in the lowermost 400 m a.g.l. ~~which can be further seen in the decline of the BC mass concentration profiles~~ BC decreased from 3.87 $\pm$0.79 to 2.51 $\pm$ 0.13 $\mu g\,m^{-3}$ in the same altitude.

~~In addition, gas concentrations of and CO were studied for the time intervals of the ALADINA flights that did not show any local emissions influence during the case study at ground. The conditions of the vortex phase on 14 July 2016, unusual during the monsoon season, included transport of aged biomass burning aerosol and decreased humidity, as described in Knippertz et al. (2017) and Flamant et al. (2018). Therefore, when comparing the case study in Sect. 3.2 and Sect. 3.3 with the mean statistics presented in Sect. 3.1, an enhanced BC concentration can be expected, which was confirmed by the observations and simulations.~~

The UAS observations were supported and spatially extended by a comparison with the model output of COSMO-ART ~~.~~ during the event. In all cases, the contribution of fresh BC to the total BC ~~is~~ was negligible in COSMO-ART, indicating that local sources ~~are~~ were not the major contributor of BC over Savè. The analysis of longitudinal vertical transects of the modelled wind speed and the BC mass concentrations ~~reveals~~ revealed that transport processes with maritime inflow from the south ~~are~~ could be the most relevant contributors of the observed BC.

This hypothesis can be supported by tracer experiments of Deroubaix et al. (2019), who showed that Savè is partly influenced by city plumes near the coast, namely Lomé, Accra and Cotonou due to maritime inflow from south. The modelled period was 1–7 July but the conditions of the vortex phase on 14 July 2016, unusual during the monsoon season, included transport of aged biomass burning aerosol and decreased humidity, as described in Knippertz et al. (2017) and Flamant et al. (2018) so that long range transport from city plumes might be the source of observed BC in Savè.

The strength of the shown study is the high capability to further understand transport processes of BC on small-scale by using UAS that are linked to regional-scale during the WAM season. However, the relationship between BC and the ABL needs more profound investigations. In addition, the impact of possible aged and transported BC within the ABL should be taken into account in future investigations that could equally contribute to a reduction of air quality and even further interact with low-level clouds.

Data availability. The data used in this study (Derrien et al., 2016; Handwerker et al., 2016; Wieser et al., 2016; Bärfuss et al., 2017) are available on the SEDOO database (http://baobab.sedoo.fr/DACCIWA/).

Author contributions. KoD and BeV provided the COSMO-ART model contributions. KaB delivered the ceilometer profiles. ChD studied the wind profiler data. FeP and CoJ were responsible for the gas concentration observations. KoB, FaP, and AsL handled the preparation and operation of the UAS, as well as the post-processing of the UAS data. FrE contributed to the statistical analysis of the UAS measurements. BiA, NoK and FaL coordinated the project, and provided access to ground observation data. BaA wrote the publication under critical review and input from all co-authors.

Competing interests. The authors declare that they have no conflict of interest.

Acknowledgements. The DACCIWA project has received funding from the European Union Seventh Framework Programme (FP7/2007-2013) under grant agreement no. 603502. BA was financially supported by the German Research Foundation (DFG) under the project number LA 2907/5-2. The authors from ~~the~~ TU Braunschweig wish to thank UPS and KIT for being part of the DACCIWA project. We gratefully acknowledge Lutz Bretschneider, Endres Kathe and Birgit Zachrau for their valuable support in preparation of the UAS ALADINA and during the experiment on site. The authors acknowledge support by the ~~German Research Foundation and the~~ Open Access Publication Funds of the Technische Universität Braunschweig. We thank both referees for their critical input and valuable suggestions for improving the manuscript.

References

Adler, B., Kalthoff, N., and Gantner, L.: Nocturnal low-level clouds over southern West Africa analysed using high-resolution simulations, Atmos. Chem. Phys., 17, 899–910, doi:10.5194/acp-17-899-2017, 2017.

Adler, B., Babić, K., Kalthoff, N., Lohou, F., Lothon, M., Dione, C., Pedruzo-Bagazgoitia, X., and Andersen, H.: Nocturnal low-level clouds in the atmospheric boundary layer over southern West Africa: an observation-based analysis of conditions and processes, Atmos. Chem. Phys., 19, 663–681, https://doi.org/10.5194/acp-19-663-2019, 2019.

Adon, A. J., Liousse, C., Doumbia, E. T., Baeza-Squiban, A., Cachier, H., Léon, J.-F., Yoboue, V., Akpo, A. B., Galy-Lacaux, C., Zoutien, C., Xu, H., Gardrat, E., and Keita, S.: Physico-chemical characterization of urban aerosols from specific combustion sources in West Africaat Abidjan in Côte d'Ivoire and Cotonou in Benin in the frame of DACCIWA program, Atmos. Chem. Phys. Discuss., https://doi.org/10.5194/acp-2019-406, in review, 2019.

Altstädter, B., Platis, A., Wehner, B., Scholtz, A., Wildmann, N., Hermann, M., Käthner, R., Baars, H., Bange, J., and Lampert, A.: ALADINA – an unmanned research aircraft for observing vertical and horizontal distributions of ultrafine particles within the atmospheric boundary layer, Atmos. Meas. Tech., 8, 1627–1639, doi:10.5194/amt-8-1627-2015, 2015.

Altstädter, B., Platis, A., Jähn, M., Baars, H., Lückerath, J., Held, A., Lampert, A., Bange, J., Hermann, M., and Wehner, B.: Airborne observations of newly formed boundary layer aerosol particles under cloudy conditions, Atmos. Chem. Phys., 18, 8249–8264, https://doi.org/10.5194/acp-18-8249-2018, 2018.

Babić, K., Adler, B., Kalthoff, N., Andersen, H., Dione, C., Lohou, F., Lothon, M., and Pedruzo-Bagazgoitia, X.: The observed diurnal cycle of low-level stratus clouds over southern West Africa: a case study, Atmos. Chem. Phys., 19, 1281–1299, https://doi.org/10.5194/acp-19-1281-2019, ~~2019.~~ 2019a.

Babić, K., Kalthoff, N., Adler, B., Quinting, J. F., Lohou, F., Dione, C., and Lothon, M.: What controls the formation of nocturnal low-level stratus clouds over southern West Africa during the monsoon season?, Atmos. Chem. Phys.~~Discuss.,~~ , 19, 13489—13506, https://doi.org/10.5194/~~acp-2019-537, in review, 2019.~~ acp-19-13489-2019, 2019b.

Baldauf, M., Seifert, A., Förstner, J., Majewski, D., Raschendorfer, M., and Reinhardt, T.: Operational convective-scale numerical weather prediction with the COSMO model: description and sensitivities, Mon. Weather Rev., 139, 3887–3905, doi:10.1175/MWR-D-10-05013.1, 2011.

Bärfuss, K., Pätzold, F., Hecker, P., and Lampert, A.: DACCIWA Savè super site. Atmospheric boundary layer properties and BC measured with the unmanned research aircraft ALADINA of the TU Braunschweig. SEDOO OMP. doi:10.6096/baobab-dacciwa.1701, 2017.

Bärfuss, K., Pätzold, F., Altstädter, B., Kathe, E., Nowak, S, Bretschneider, L., Bestmann, U., and Lampert, A.: New Setup of the UAS ALADINA for Measuring Boundary Layer Properties, Atmospheric Particles and Solar Radiation, Atmosphere, 9, 1–21, https://doi.org/10.3390/atmos9010028, 2018.

Båserud, L., Reuder, J., Jonassen, M. O., Kral, S. T., Paskyabi, M. B., and Lothon, M.: Proof of concept for turbulence measurements with the RPAS SUMO during the BLLAST campaign, Atmos. Meas. Tech., 9, 4901–4913, https://doi.org/10.5194/amt-9-4901-2016, 2016.

~~Bessardon, G., Brooks, B., Abiye, O., Adler, B., Ajao, A., Ajileye, O., Altstädter, B., Amekudzi, L. K., Aryee, J. N. A., Atiah, W. A., Ayoola, M., Babić, K., Bärfuss, K., Bezombes, Y., Bret, G., Brilouet, P.-E., Cayle-Aethelhard, F., Danuor, S., Delon, C., Derrien, S., Dione, C., Durand, P., Fosu-Amankwah, K., Gabella, O., Groves, J., Handwerker, J., Kalthoff, N., Kohler, M., Kunka, N., Jambert, C., Jegede, G., Lampert, A., Leclercq, J., Lohou, F., Lothon, M., Medina, P., Pätzold, F., Pedruzo Bagazgoitia, X., Reinares, I., Sharpe, S., Smith, V.,~~

~~Sunmonu, L. A., Tan, N., and Wieser, A.: A dataset of the 2016 monsoon season meteorology in southern West Africa – an overview from the DACCIWA campaign, Sci. Data, in review, 2018.~~

Bond, T. C., Doherty, S. J., Fahey, D. W., Forster, P. M., Berntsen, T., DeAngelo, B. J., Flanner, M. G., Ghan, S., Karcher, B., Koch, D., Kinne, S., Kondo, Y., Quinn, P. K., Sarofim, M. C., Schultz, M. G., Schulz, M., Venkataraman, C., Zhang, H., Zhang, S., Bellouin, N., Guttikunda, S. K., Hopke, P. K., Jacobson, M. Z., Kaiser, J. W., Klimont, Z., Lohmann, U., Schwarz, J. P., Shindell, D., Storelvmo, T., Warren, S. G., and Zender, C. S.: Bounding the role of black carbon in the climate system: A scientific assessment, J. Geophys. Res.-Atmos., 118, 5380–5552, doi:10.1002/Jgrd.50171, 2013.

Brosy, C., Krampf, K., Zeeman, M., Wolf, B., Junkermann, W., Schäfer, K., Emeis, S., and Kunstmann, H.: Simultaneous multicopter-based air sampling and sensing of meteorological variables, Atmos. Meas. Tech., 10, 2773–2784, https://doi.org/10.5194/amt-10-2773-2017, 2017.

Brito, J., Freney, E., Dominutti, P., Borbon, A., Haslett, S. L., Batenburg, A. M., Colomb, A., Dupuy, R., Denjean, C., Burnet, F., Bourriane, T., Deroubaix, A., Sellegri, K., Borrmann, S., Coe, H., Flamant, C., Knippertz, P., and Schwarzenboeck, A.: Assessing the role of anthropogenic and biogenic sources on PM1 over southern West Africa using aircraft measurements, Atmos. Chem. Phys., 18, 757–772, https://doi.org/10.5194/acp-18-757-2018, 2018.

Corrigan, C. E., Roberts, G. C., Ramana, M. V., Kim, D., and Ramanathan, V.: Capturing vertical profiles of aerosols and black carbon over the Indian Ocean using autonomous unmanned aerial vehicles, Atmos. Chem. Phys., 8, 737–747, doi:10.5194/acp-8-737-2008, 2008.

Chiliński, M. T., Markowicz, K. M. and Kubicki, M.: UAS as a Support for Atmospheric Aerosols Research: Case Study, Pure Appl. Geophys., 175, 3325–3342, doi:10.1007/s00024-018-1767-3, 2018.

Collaud Coen, M., Weingartner, E., Apituley, A., Ceburnis, D., Fierz-Schmidhauser, R., Flentje, H., Henzing, J. S., Jennings, S. G., Moerman, M., Petzold, A., Schmid, O., and Baltensperger, U.: Minimizing light absorption measurement artifacts of the Aethalometer: evaluation of five correction algorithms, Atmos. Meas. Tech., 3, 457-–474, doi:10.5194/amt-3-457-2010, 2010.

Cuxart, J., Wrenger, B., Martínez-Villagrasa, D., Reuder, J., Jonassen, M. O., Jiménez, M. A., Lothon, M., Lohou, F., Hartogensis, O., Dünnermann, J., Conangla, L., and Garai, A.: Estimation of the advection effects induced by surface heterogeneities in the surface energy budget, Atmos. Chem. Phys., 16, 9489–9504, doi:10.5194/acp-16-9489-2016, 2016.

Deetz, K., Vogel, H., Knippertz, P., Adler, B., Taylor, J., Coe, H., Bower, K., Haslett, S., Flynn, M., Dorsey, J., Crawford, I., Kottmeier, C., and Vogel, B.: Numerical simulations of aerosol radiative effects and their impact on clouds and atmospheric dynamics over southern West Africa, Atmos. Chem. Phys., 18, 9767-–9788, https://doi.org/10.5194/acp-18-9767-2018, 2018.

Deroubaix, A., Menut, L., Flamant, C., Brito, J., Denjean, C., Dreiling, V., Fink, A., Jambert, C., Kalthoff, N., Knippertz, P., Ladkin, R., Mailler, S., Maranan, M., Pacifico, F., Piguet, B., Siour, G., and Turquety, S.: Diurnal cycle of coastal anthropogenic pollutant transport over southern West Africa during the DACCIWA campaign, Atmos. Chem. Phys., 19, 473–497, https://doi.org/10.5194/acp-19-473-2019, 2019.

Derrien, S., Bezombes, Y., Bret, G., Gabella, O., Jarnot, C., Medina, P., Piques, E., Delon, C., Dione, C., Cambistron, B., Durand, P., Jambert, C., Lohou, F., Lothon, M., Pacifico, F., and Meyerfeld, Y.: DACCIWA field campaign, Savè super-site, UPS instrumentation. SEDOO OMP, doi:10.6096/dacciwa.1618, 2016.

Dione, C., Lohou, F., Lothon, M., Adler, B., Babić, K., Kalthoff, N., Pedruzo-Bagazgoitia, X., Bezombes, Y., and Gabella, O.: ~~Low Level Cloud and Dynamical Features within the Southern West African Monsoon~~Low-level stratiform clouds and dynamical features observed within the southern West African monsoon, Atmos. Chem. Phys.~~Discuss.,~~ , 19, 8979–8997, https://doi.org/10.5194/~~acp-2018-1149, in review, 2018.~~ acp-19-8979-2019, 2019.

Ferrero, L., Castelli, M., Ferrini, B. S., Moscatelli, M., Perrone, M. G., Sangiorgi, G., D'Angelo, L., Rovelli, G., Moroni, B., Scardazza, F., Močnik, G., Bolzacchini, E., Petitta, M., and Cappelletti, D.: Impact of black carbon aerosol over Italian basin valleys: high-resolution measurements along vertical profiles, radiative forcing and heating rate, Atmos. Chem. Phys., 14, 9641–9664, https://doi.org/10.5194/acp-14-9641-2014, 2014.

Flamant, C., Knippertz, P., Fink, A. H., Akpo, A., Brooks, B., Chiu, C. J., Coe, H., Danuor, S., Evans, M., Jegede, O., Kalthoff, N., Konaré, A., Liousse, C., Lohou, F., Mari, C., Schlager, H., Schwarzenboeck, A., Adler, B., Amekudzi, L., Aryee, J., Ayoola, M., Batenburg, A. M., Bessardon, G., Borrmann, S., Brito, J., Bower, K., Burnet, F., Catoire, V., Colomb, A., Denjean, C., Fosu-Amankwah, K. , Hill, P. G., Lee, J., Lothon, M., Maranan, M., Marsham, J., Meynadier, R., Ngamini, J., Rosenberg, P., Sauer, D., Smith, V., Stratmann, G., Taylor, J. W., Voigt, C., and V. Yoboué: The Dynamics–Aerosol–Chemistry–Cloud Interactions in West Africa Field Campaign: Overview and Research Highlights, Bull. Amer. Meteor. Soc., 99, 83—104, https://doi.org/10.1175/BAMS-D-16-0256.1, 2018.

Gounou, A., Guichard, F., and Couvreux, F.: Observations of diurnal cycles over a West African meridional transect: Pre-monsoon and full-monsoon seasons, Bound.-Layer Meteor., 144, 329–357, doi:10.1007/s10546-012-9723-8, 2012.

Handwerker, J., Scheer, S., and Gamer, T.: DACCIWA field campaign, Savè super-site, Cloud and precipitation. SEDOO OMP,, https://doi.org/10.6096/DACCIWA.1686, 2016.

Hannak, L., Knippertz, P., Fink. A. H., Kniffka, A., and Pante, G.: Why Do Global Climate Models Struggle to Represent Low-Level Clouds in the West African Summer Monsoon?, J. Climate, 30, 1665–1687, doi:10.1175/JCLI-D-16-0451.1, 2017.

Hansen, A. D. A., Rosen, H., and Novakov, T.: The aethalometer–an instrument for the real-time measurement of optical absorption by aerosol particles, Sci. Total Environ., 36, 191–196, 1984.

Hansen, J., Sato, M., and Ruedy, R.: Radiative forcing and climate response, J. Geophys. Res., 102, 6831–6864, doi:10.1029/96JD03436, 1997.

Huang, J., Adams, A., Wang, C., and Zhang, C.: Black carbon and West African Monsoon precipitation: observations and simulations, Ann. Geophys., 27, 4171–4181, doi:www.ann-geophys.net/27/4171/2009/, 2009.

Jiménez, M. A., Simó, G, Wrenger, B., Telisman-Prtenjak, M., Guijarro, J. A., and Cuxart, J.: Morning transition case between the land and the sea breeze regimes, Atmos. Res., 172–173, 95–108, https://doi.org/10.1016/j.atmosres.2015.12.019, 2016.

Kalthoff, N., Lohou, F., Brooks, B., Jegede, G., Adler, B., Babić, K., Dione, C., Ajao, A., Amekudzi, L. K., Aryee, J. N. A., Ayoola, M., Bessardon, G., Danuor, S. K., Handwerker, J., Kohler, M., Lothon, M., Pedruzo-Bagazgoitia, X., Smith, V., Sunmonu, L., Wieser, A., Fink, A. H., and Knippertz, P.: An overview of the diurnal cycle of the atmospheric boundary layer during the West African monsoon season: results from the 2016 observational campaign, Atmos. Chem. Phys., 18, 2913–2928, https://doi.org/10.5194/acp-18-2913-2018, 2018.

Knippertz, P., Fink, A. H., Schuster, R., Trentmann, J., Schrage, J. M., and Yorke, C.: Ultra-low clouds over the southern West African monsoon region, Geophys. Res. Lett., 38, L21808, 1–7, doi: 10.1029/2011GL049278, 2011.

Knippertz, P., Evans, M. J., Field, P. R., Fink, A. H., Liousse, C., and Marsham, J. H.: The possible role of local air pollution in climate change in West Africa, Nat. Clim. Change, 5, 815–822, doi:10.1038/NCLIMATE2727, 2015a.

Knippertz, P., Coe, H., Chiu, J. C., Evans, M. J., Fink, A. H., Kalthoff, N., Liousse, C., Mari, C., Allan, R. P., Brooks, B., Danour, S., Flamant, C., Jegede, O. O., Lohou, F., and Marsham, J. H.: The DACCIWA project: Dynamics-aerosol-chemistry-cloud interactions in West Africa, Bull. Amer. Meteor. Soc., 96, 1451–1460, https://doi.org/10.1175/BAMS-D-14-00108.1, 2015b.

Knippertz, P., Fink, A. H., Deroubaix, A., Morris, E., Tocquer, F., Evans, M. J., Flamant, C., Gaetani, M., Lavaysse, C., Mari, C., Marsham, J. H., Meynadier, R., Affo-Dogo, A., Bahaga, T., Brosse, F., Deetz, K., Guebsi, R., Latifou, I., Maranan, M., Rosenberg, P. D., and Schlueter, A.: A meteorological and chemical overview of the DACCIWA field campaign in West Africa in June—July 2016, Atmos. Chem. Phys., 17, 10893–10918, https://doi.org/10.5194/acp-17-10893-2017, 2017.

Lee, J.: Performance Test of MicroAeth® AE51 at Concentrations Lower than $2\,\mu g\,m^{-3}$ in Indoor Laboratory, Appl. Sci., 9, 1–14, doi:10.3390/app9132766, 2019.

Li, Z., Liu, J., Mauzerall, D. L., Li, X., Fan, S., Horowitz, L. W., He, C., Yi, K., and Tao, S.: A potential large and persistent black carbon forcing over Northern Pacific inferred from satellite observations, Sci. Rep., 7, 43429, 1–8, doi:10.1038/srep43429, 2017.

Liousse, C., Assamoi, E., Criqui, E. P., Granier, C., and Rosset, R.: Explosive growth in African combustion emissions from 2005 to 2030, Environ. Res. Lett., 9, 035003, 1–10, doi:10.1088/1748-9326/9/3/035003, 2014.

Liu, B., Ma, Y., Gong, W., Zhang, M., and Shi, Y.: The relationship between black carbon and atmospheric boundary layer height, Atmos. Pollut. Res., 10, 65-–72, https://doi.org/10.1016/j.apr.2018.06.007, 2018.

Mari, C. H., Cailley, G., Corre, L., Saunois, M., Attié, J. L., Thouret, V., and Stohl, A.: Tracing biomass burning plumes from the Southern Hemisphere during the AMMA 2006 wet season experiment, Atmos. Chem. Phys., 8, 3951—3961, https://doi.org/10.5194/acp-8-3951-2008, 2008.

Marino, M., Fisher, A., Clothier, R., Watkins, S., Prudden, S., and Leung, C. S.: An Evaluation of Multi-Rotor Unmanned Aircraft as Flying Wind Sensors, Int. J. Mirco Air Veh., 7, 285–299, https://doi.org/10.1260/1756-8293.7.3.285, 2015.

Mayer, S., Sandvik, A., Jonassen, M., and Reuder, J.: Atmospheric profiling with the UAS SUMO: a new perspective for the evaluation of fine-scale atmospheric models, Meteorol. Atmos. Phys., 116, 15–26, doi:10.1007/s00703-010-0063-2, 2010.

Platis, A., Altstädter, B., Wehner, B., Wildmann, N., Lampert. A., Hermann, M., Birmili, W., and Bange, J.: An observational case study on the influence of atmospheric boundary layer dynamics on the new particle formation, Bound.-Lay. Meteorol., 158, 67–92, doi:10.1007/s10546-015-0084-y, 2016.

Pacifico, F., Delon, C., Jambert, C., Durand, P., Morris, E., Evans, M. J., Lohou, F., Derrien, S., Donnou, V. H. E., Houeto, A. V., Reinares ~~Martinez~~Martínez, I., and Brilouet, P.-E.: Measurements of nitric oxide and ammonia soil fluxes from a wet savanna ecosystem site in West Africa during the DACCIWA field campaign, Atmos. Chem. Phys.~~Discuss.,~~, 19, 2299—2325, https://doi.org/10.5194/~~acp-2017-1198, in review, 2018.~~ acp-19-2299-2019, 2019.

Petäjä, T., Järvi, L., Kerminen, V. M., Ding, A. J., Sun, J. N., Nie, W., Kujansuu, J., Virkkula, A., Yang, X., Fu, C. B., Zilitinkevich, S., and Kulmala, M.: Enhanced air pollution via aerosol-boundary layer feedback in China, Sci. Rep., 6, 18998, doi:10.1038/srep18998, 2016.

Petzold, A., Ogren, J. A., Fiebig, M., Laj, P., Li, S.-M., Baltensperger, U., Holzer-Popp, T., Kinne, S., Pappalardo, G., Sugimoto, N., Wehrli, C., Wiedensohler, A., and Zhang, X.-Y.: Recommendations for reporting "black carbon" measurements, Atmos. Chem. Phys., 13, 8365—8379, https://doi.org/10.5194/acp-13-8365-2013, 2013.

Pikridas, M., Bezantakos, S., Močnik, G., Keleshis, C., Brechtel, F., Stavroulas, I., Demetriades, G., Antoniou, P., Vouterakos, P., Argyrides, M., Liakakou, E., Drinovec, L., Marinou, E., Amiridis, V., Vrekoussis, M., Mihalopoulos, N., and Sciare, J.: On-flight intercomparison of three miniature aerosol absorption sensors using unmanned aerial systems (UASs), Atmos. Meas. Tech., 12, 6425—6447, https://doi.org/10.5194/amt-12-6425-2019, 2019.

Ran, L., Deng, Z., Xu, X., Yan, P., Lin, W., Wang, Y., Tian, P., Wang, P., Pan, W., and Lu, D.: Vertical profiles of black carbon measured by a micro-aethalometer in summer in the North China Plain, Atmos. Chem. Phys., 16, 10441–10454, https://doi.org/10.5194/acp-16-10441-2016, 2016.

Renard, J.-B., Dulac, F., Berthet, G., Lurton, T., Vignelles, D., Jégou, F., Tonnelier, T., Jeannot, M., Couté, B., Akiki, R., Verdier, N., Mallet, M., Gensdarmes, F., Charpentier, P., Mesmin, S., Duverger, V., Dupont, J.-C., Elias, T., Crenn, V., Sciare, J., Zieger, P., Salter, M., Roberts, T., Giacomoni, J., Gobbi, M., Hamonou, E., Olafsson, H., Dagsson-Waldhauserova, P., Camy-Peyret, C., Mazel, C., Décamps, T., Piringer, M., Surcin, J., and Daugeron, D.: LOAC: a small aerosol optical counter/sizer for ground-based and balloon measurements of the size distribution and nature of atmospheric particles – Part 2: First results from balloon and unmanned aerial vehicle flights, Atmos. Meas. Tech., 9, 3673–3686, doi:10.5194/amt-9-3673-2016, 2016.

Riemer, N., Vogel, H., and Vogel, B.: Soot aging time scales in polluted regions during day and night, Atmos. Chem. Phys., 4, 1885–1893, doi:10.5194/acp-4-1885-2004, 2004.

Saturno, J., Pöhlker, C., Massabò, D., Brito, J., Carbone, S., Cheng, Y., Chi, X., Ditas, F., Hrabě de Angelis, I., Morán-Zuloaga, D., Pöhlker, M. L., Rizzo, L. V., Walter, D., Wang, Q., Artaxo, P., Prati, P., and Andreae, M. O.: Comparison of different Aethalometer correction schemes and a reference multi-wavelength absorption technique for ambient aerosol data, Atmos. Meas. Tech., 10, 2837–2850, https://doi.org/10.5194/amt-10-2837-2017, 2017.

Stockwell, W. R., Middleton, P., Chang, J. S., and Tang, X.: The second generation regional acid deposition model chemical mechanism for regional air quality modeling, J. Geophys. Res.-Atmos., 95, 16343–16367, doi:10.1029/JD095iD10p16343, 1990.

Virkkula, A., Mäkelä, T., Hillamo, R., Yli-Tuomi, T., Hirsikko, A., Hämeri, K., and Koponen, I. K.: A simple procedure for correcting loading effects of aethalometer data, J. Air Waste Manage., 57, 1214—1222, doi:10.3155/1047-3289.57.10.1214, 2007.

Vogel, B., Vogel, H., Bäumer, D., Bangert, M., Lundgren, K., Rinke, R., and Stanelle, T.: The comprehensive model system COSMO-ART–Radiative impact of aerosol on the state of the atmosphere on the regional scale, Atmos. Chem. Phys., 9, 8661–8680, https://doi.org/10.5194/acp-9-8661-2009, 2009.

Weingartner, E., Saathoff, H., Schnaiter, M., Streit, N., Bitnar, B., and Baltensperger, U.: Absorption of light by soot particles: determination of the absorption coefficient by means of aethalometers, J. Aerosol Sci., 34, 1445-–1463, doi:10.1016/S0021-8502(03)00359-8, 2003.

Wilcox, E. M., Thomas, R. M., Praveen, P. S., Pistone, K., Bender, F. A., and Ramanathan, V.: Black carbon solar absorption suppresses turbulence in the atmospheric boundary layer, P. Natl. Acad. Sci. USA, 113, 11794—11799, https://doi.org/10.1073/pnas.1525746113, 2016.

Wieser, A., Adler, B., and Deny, B.: “DACCIWA field campaign, Savè super-site, Thermodynamic data sets.” SEDOO OMP. doi: 10.6096/dacciwa.1659, 2016.

Wildmann, N., Mauz, M., and Bange, J.: Two fast temperature sensors for probing of the atmospheric boundary layer using small remotely piloted aircraft (RPA), Atmos. Meas. Tech., 6, 2101–2113, doi:10.5194/amt-6-2101-2013, 2013.

Wildmann, N., Ravi, S., and Bange, J.: Towards higher accuracy and better frequency response with standard multi-hole probes in turbulence measurements with remotely piloted aircraft (RPA), Atmos. Meas. Tech., 7, 1027—1041, doi:10.5194/amt-7-1027-2014, 2014.

Zhang, R. Y., Khalizov, A. F., Pagels, J., Zhang, D., Xue, H. X., and McMurry, P. H.: Variability in morphology, hygroscopicity, and optical properties of soot aerosols during atmospheric processing, P. Natl. Acad. Sci. USA, 105, 10291—10296, doi:10.1073/pnas.0804860105, 2008.

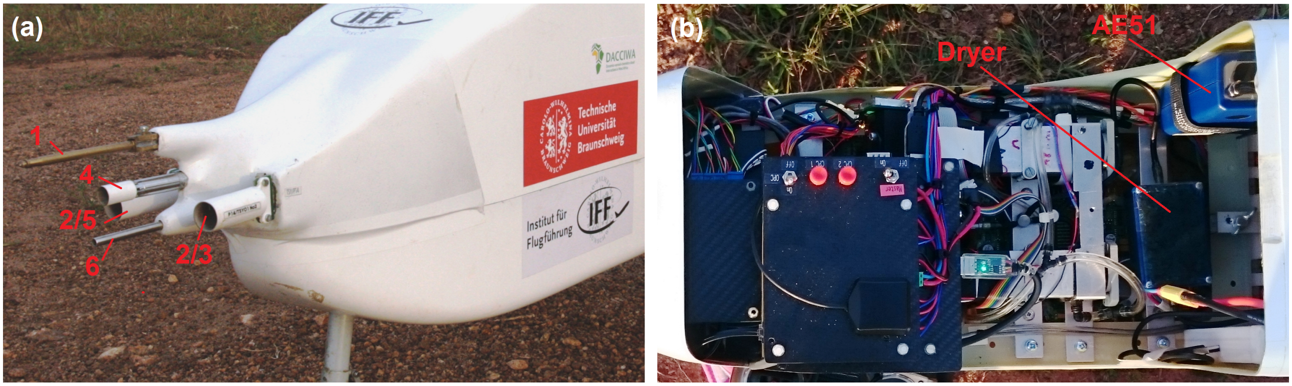

Figure 1. (a) The nose of the ~~aircraft~~ UAS ALADINA is equipped with meteorological sensors for calculating the three dimensional wind vector with one multihole probe (number 1), the temperature (number 2–4) and the humidity (number 4 and 5). The air probe is sampled with one aerosol inlet (number 6) mounted at the tip of the aircraft's nose. (b) The micro aethalometer AE51 is installed in the front compartment of the aircraft for adjusting the centre of gravity. The air stream is dried with silica gel before measuring (see the blue box close to the AE51). © Institute of Flight Guidance, TU Braunschweig.

~~The unmanned aerial system ALADINA before take off during the DACCIWA experiment at the local airfield of Savè. © Institute of Flight Guidance, TU Braunschweig.~~

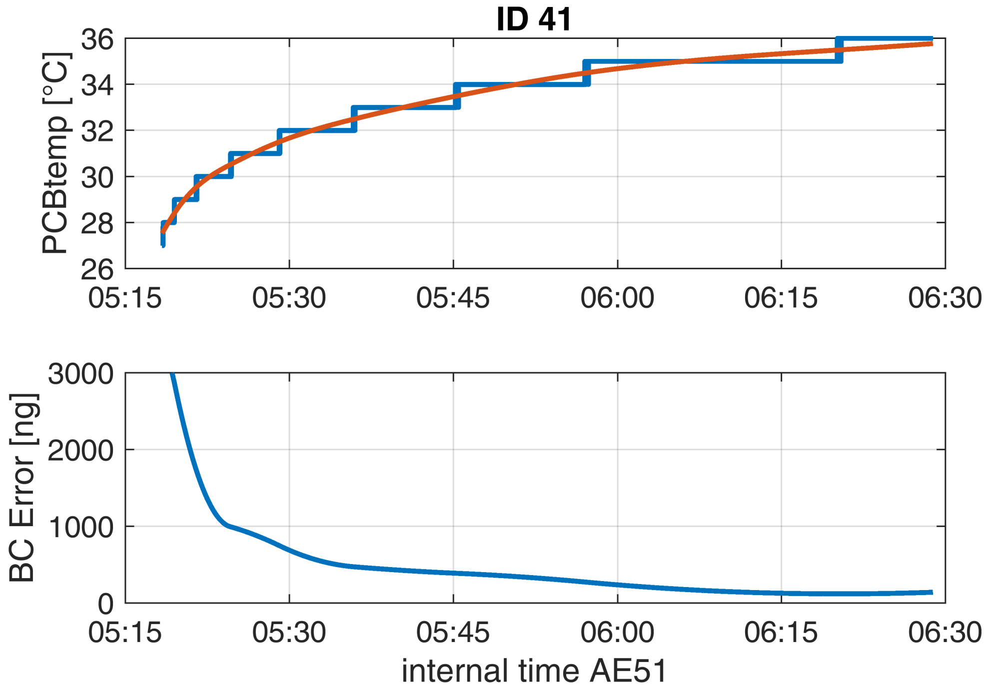

Figure 2. The impact of the temperature changes on the BC mass concentration. The figure shows the internal temperature (PCBtemp) of the aethalometer AE51 during the measurement flight on 14 July 2016 from 05:16 until 06:30 UTC (top). The bit noise was smoothed for the time interval (red line). The figure at the bottom represents the calculated error of the black carbon mass concentration.

~~Power spectra of (a) the wind vector components~~ $\cancel{u}$ ~~(green line),~~ $\cancel{v}$ ~~(blue line) and~~ $\cancel{w}$ ~~(black line) derived from the multi hole probe and (b) potential temperature~~ $\cancel{\theta}$ ~~(red line) after complimentary filtering of the slow and fast temperature sensors. The green dashed line represents the Kolmogorov law with a slope of~~ $\cancel{^{-5/3}}$~~. The data was derived from a horizontal flight at the constant height of~~ $\cancel{100 \pm 1.5}$ ~~m a.s.l. on 2 July 2016.~~

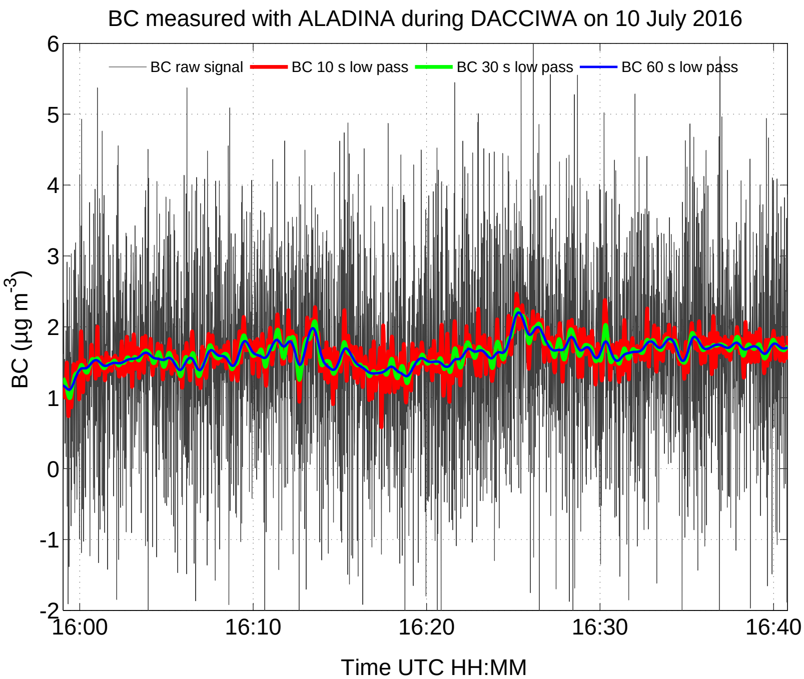

Figure 3. The BC mass concentration measured during one flight between 15:58 and 16:42 UTC on 10 July 2016. The raw signal of BC (grey line) was phase shift free low pass filtered after post-processing with 10 s (red line), 30 s (green line) and 60 s (blue line).

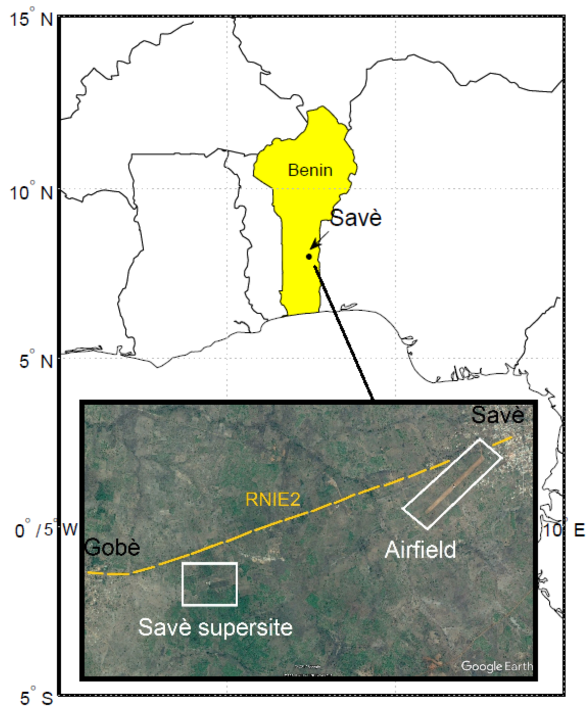

Figure 4. The map shows the position of the measurement site Savè in Benin (marked in yellow), West Africa. The UAS ALADINA was operated at the local airfield of Savè during the field experiment DACCIWA from 2 until 16 July 2016. The Savè supersite of Karlsruhe Institute of Technology (KIT) and Université de Tolouse III- Paul Sabatier (UPS) was located in the south-west with a distance of 4 km to the airfield. The sites are connected via the main road RNIE2 (dashed yellow line). The picture was created with **Google Earth** on 28 April 2017.

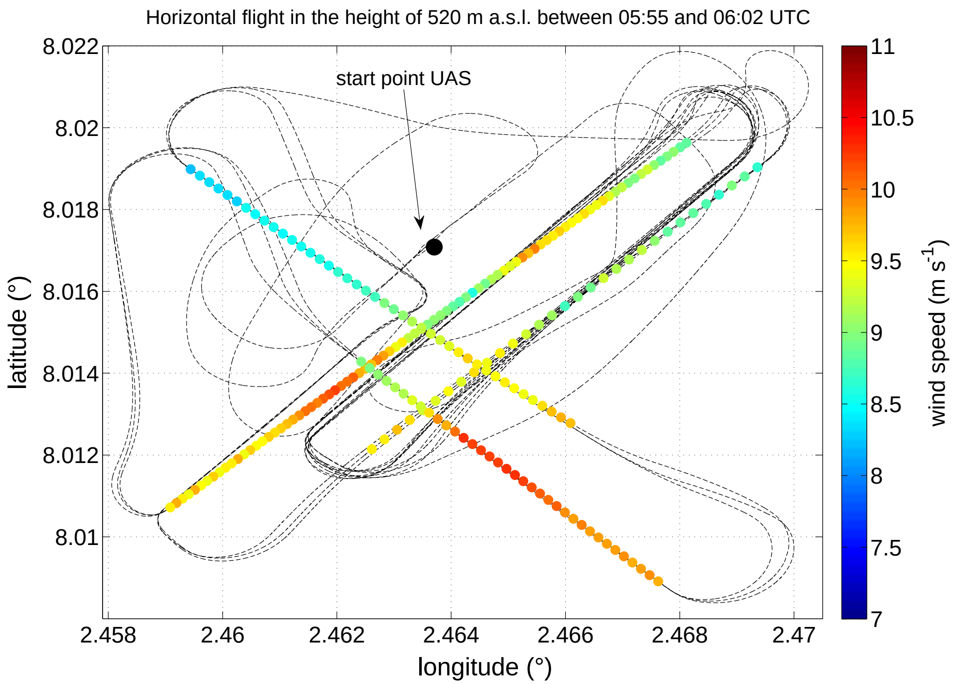

Figure 5. A typical flight pattern of ALADINA (black line) during DACCIWA. The start position of the UAS is marked with a black dot. The colour bar indicates the wind speed of four horizontal legs in the constant height of 520 m a.s.l on 14 July 2016. The horizontal flights were orientated towards the Savè supersite and the pattern were flown parallel and perpendicular to the current wind direction. The wind speed varied between 7 and 11 $\mathrm{m\,s^{-1}}$ and shows larger wind speeds heading to the south.

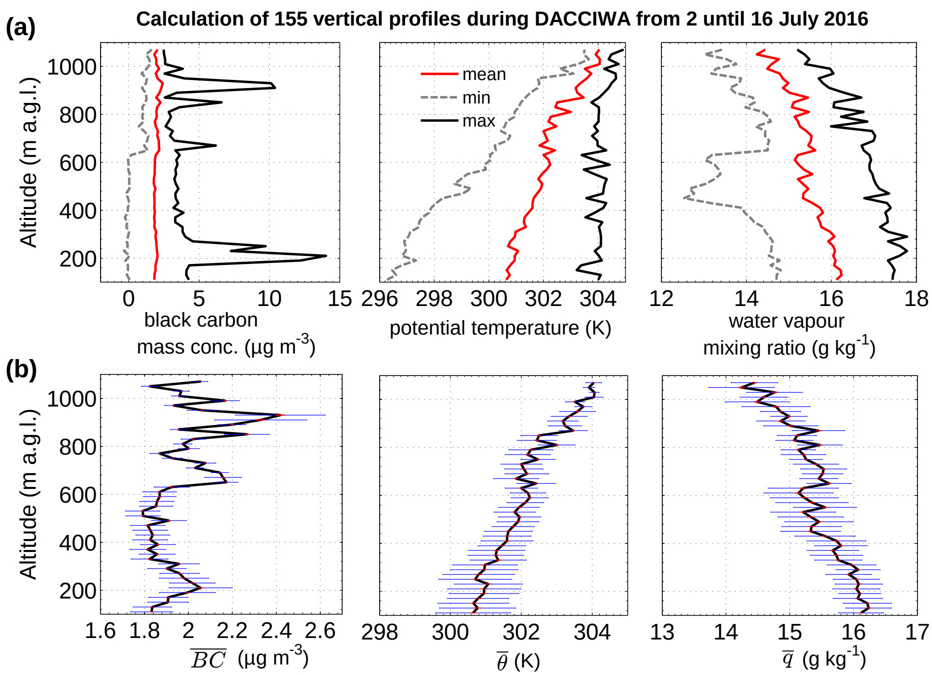

Figure 6. Summary of 155 vertical profiles from 100 to 1100 m a.g.l. measured with ALADINA during the field experiment of DACCIWA lasting from 2 until 16 July 2016. From left to right: Vertical profiles of black carbon mass concentration (BC) measured with the aethalometer and 10 s low pass filtering, potential temperature θ and water vapour mixing ratio q. The red line represents the mean value, the grey dashed lines stands for the total minimum and the black solid line is the total maximum of all vertical profiles, averaged in 20 m altitude intervals. At the bottom: The mean values of BC ($\overline{BC}$), θ ($\bar{\theta}$) and q ($\bar{q}$) in the 20 m steps, and the corresponding standard deviation for each height interval.

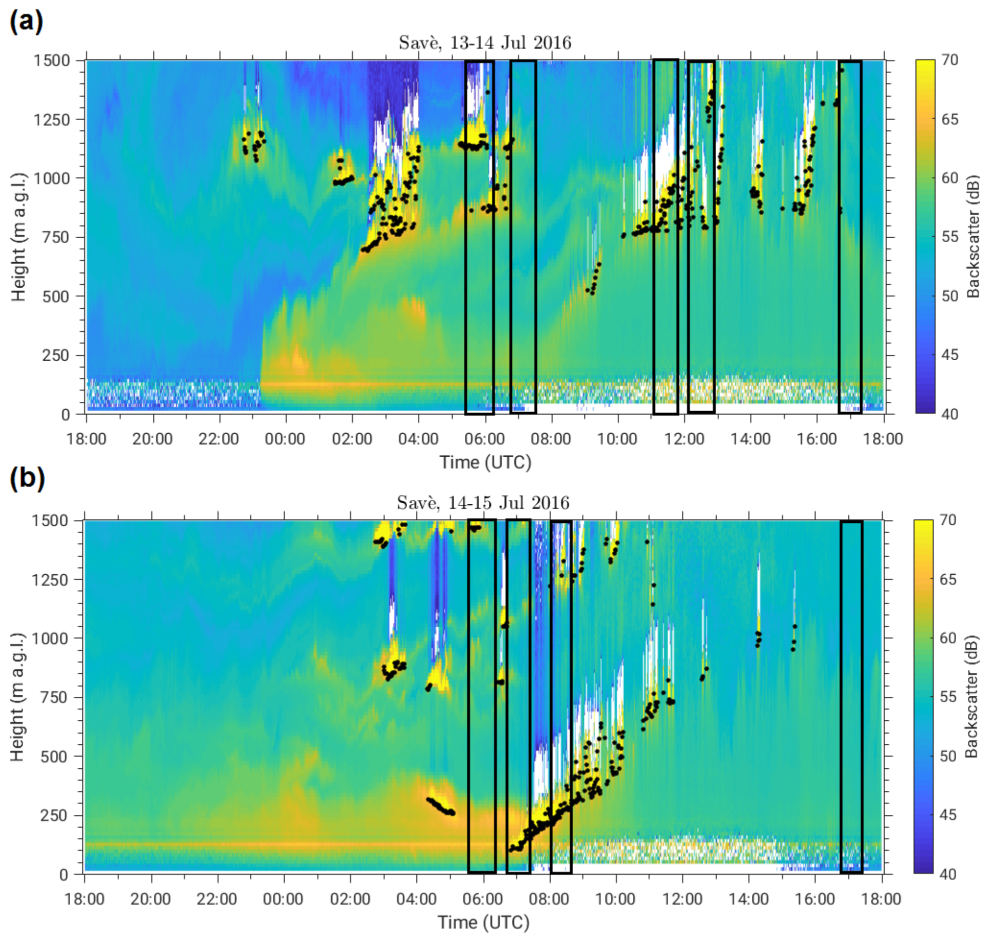

Figure 7. Backscatter signal of KIT ceilometer (Handwerker et al., 2016) installed at Savè supersite between (a) 18:00 UTC on 13 July 2016 and 18:00 UTC on 14 July 2016 and (b) in the period of 18:00 UTC on July 14 2016–18:00 UTC on July 15 2016. On July 14, different layers of atmospheric particles were observed during the day. At midday, clouds were detected at 800 m a.g.l. and dissolved at 18:00 UTC. On July 15, low-level clouds occurred at 07:00 UTC in the lowermost 200 m a.g.l., lifted up to the height of 750 m a.g.l. at 11:00 UTC and dissolved in the afternoon at 14:00 UTC in the lowermost 1.5 km. The black boxes indicate the flight periods of the UAS ALADINA.

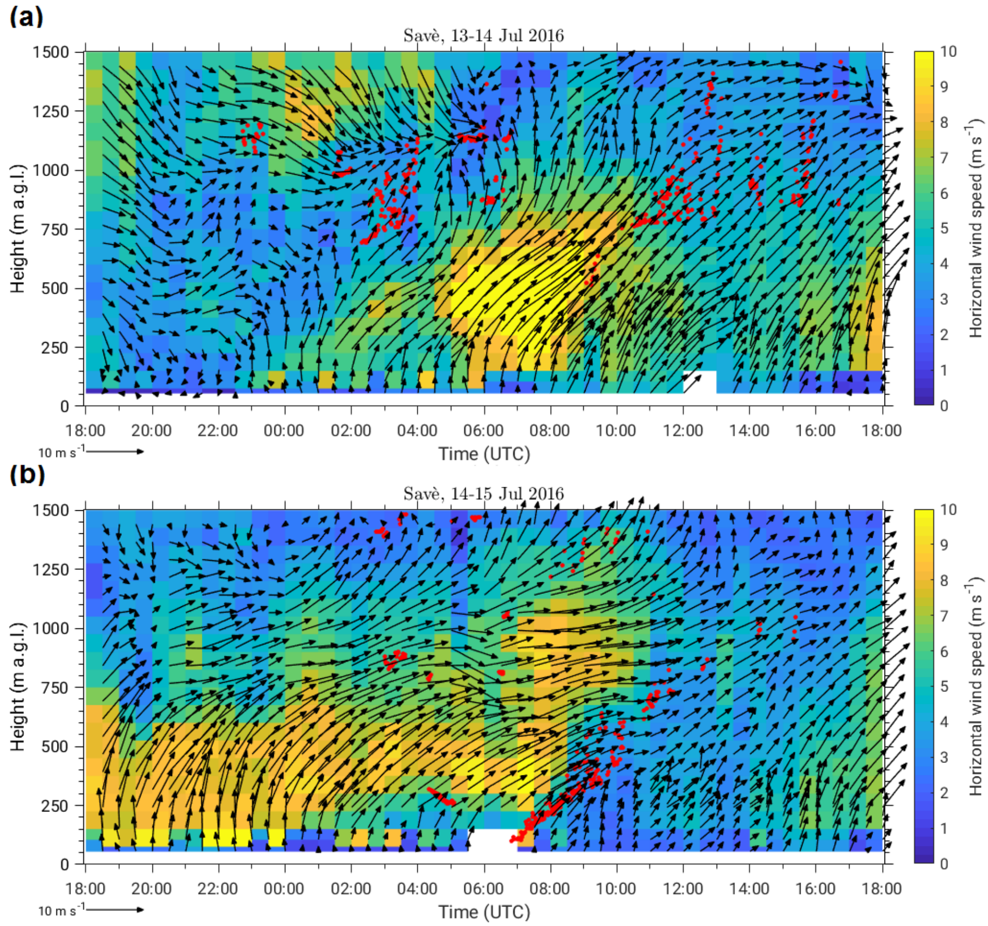

Figure 8. Time series of the wind speed and the wind direction at Savè supersite during DACCIWA (Derrien et al., 2016). The wind speed is indicated in the colour bar and the direction in arrows (a leftwards horizontal arrow stands for wind direction from E; from bottom to top for S wind). The wind speed in the lowermost 1.5 km was measured with the wind profiler of UPS between (a) 18:00 UTC on 13 July 2016 until 18:00 UTC on 14 July 2016 and (b) from 18:00 UTC on 14 July 2016–18:00 UTC on 15 July 2016. The red dots display the cloud base height measured with the ceilometer.

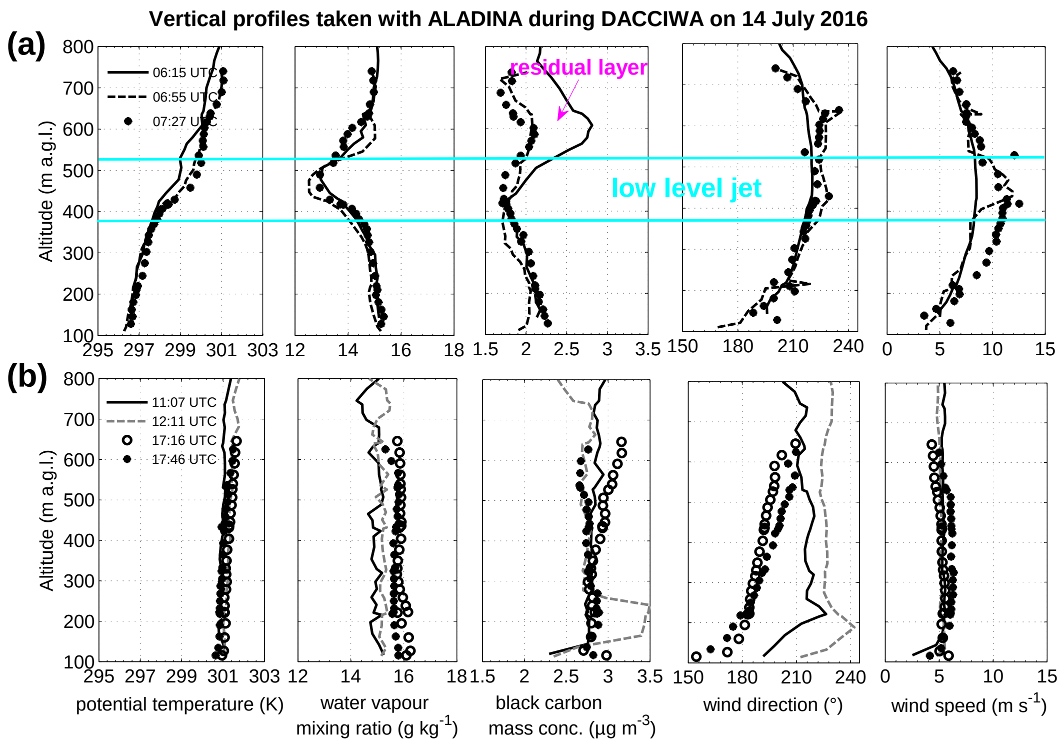

Figure 9. Vertical profiles taken with ALADINA between the height of 100 and 800 m a.g.l. on 14 July 2016. From left to right: potential temperature, water vapour mixing ratio, black carbon mass concentration, wind direction and wind speed (a) in the morning from 06:16 until 07:27 UTC and (b) during the cloud formation below the height of 800 m a.g.l. at 11:07 and 12:11 UTC and during the evening transition at 17:16 and 17:46 UTC. The horizontal turquoise line indicates the altitude range of the ~~NLLJ~~ nocturnal low-level jet (see Fig. 8a).

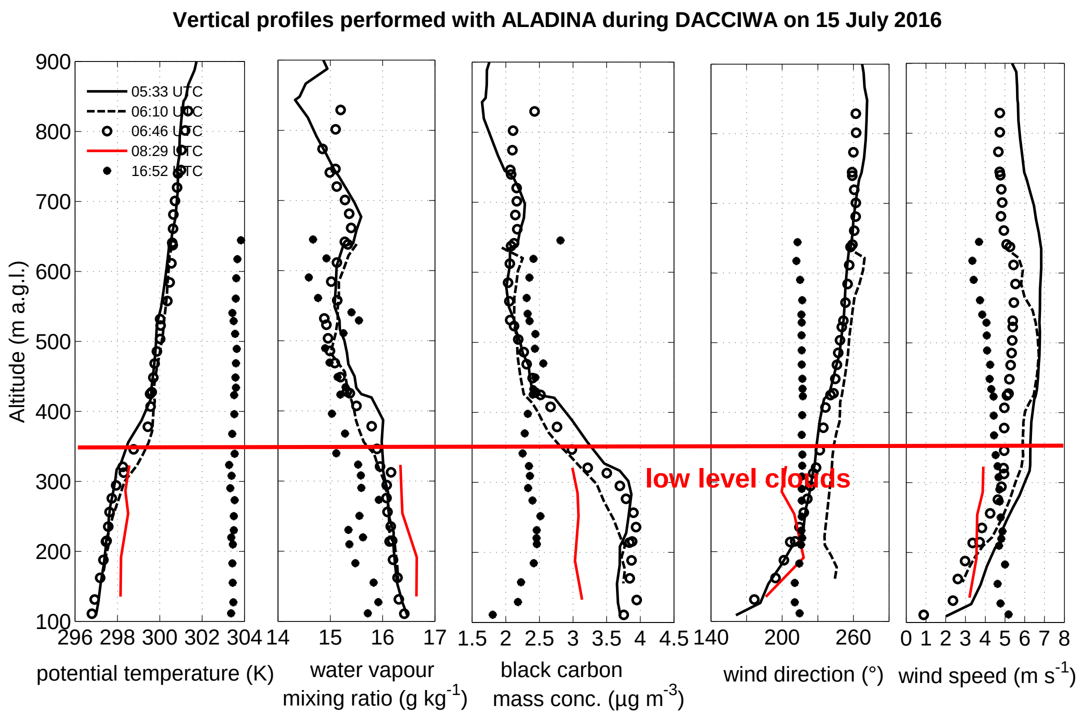

Figure 10. Five selected vertical profiles measured with ALADINA between the height of 100 and 900 m a.g.l. from 05:33 until 16:52 UTC on 15 July 2016. From left to right: potential temperature, water vapour mixing ratio, black carbon mass concentration, wind direction and wind speed. The red horizontal line shows the altitude of ~~the~~ low-level clouds ~~(LLC)~~ formed at 07:00 UTC, derived from the backscatter signal of the ceilometer (see Fig. 7b).

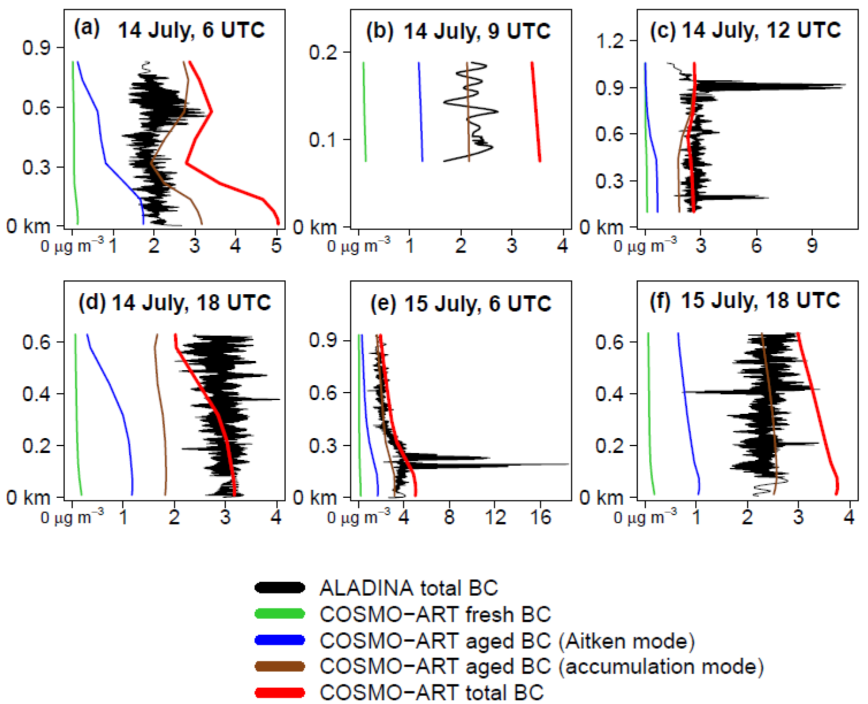

Figure 11. Vertical profiles of BC in $\mu g\,m^{-3}$ at Savè for (a–d) 14 July 2016 and (e–f) 15 July 2016. The ALADINA observations of the total BC are denoted in black, the COSMO-ART results for fresh BC, aged BC (Aitken mode), aged BC (accumulation mode) and the total BC are shown in green, blue, brown and red, respectively. The observations were temporally assigned to the three hourly model output with a deviation not larger than 1 h and by subsequently interpolating the model data to the ALADINA altitudes. Within these time steps, ALADINA conducted several ascents and descents. It is assumed that the observations within the time steps are measured instantaneously.

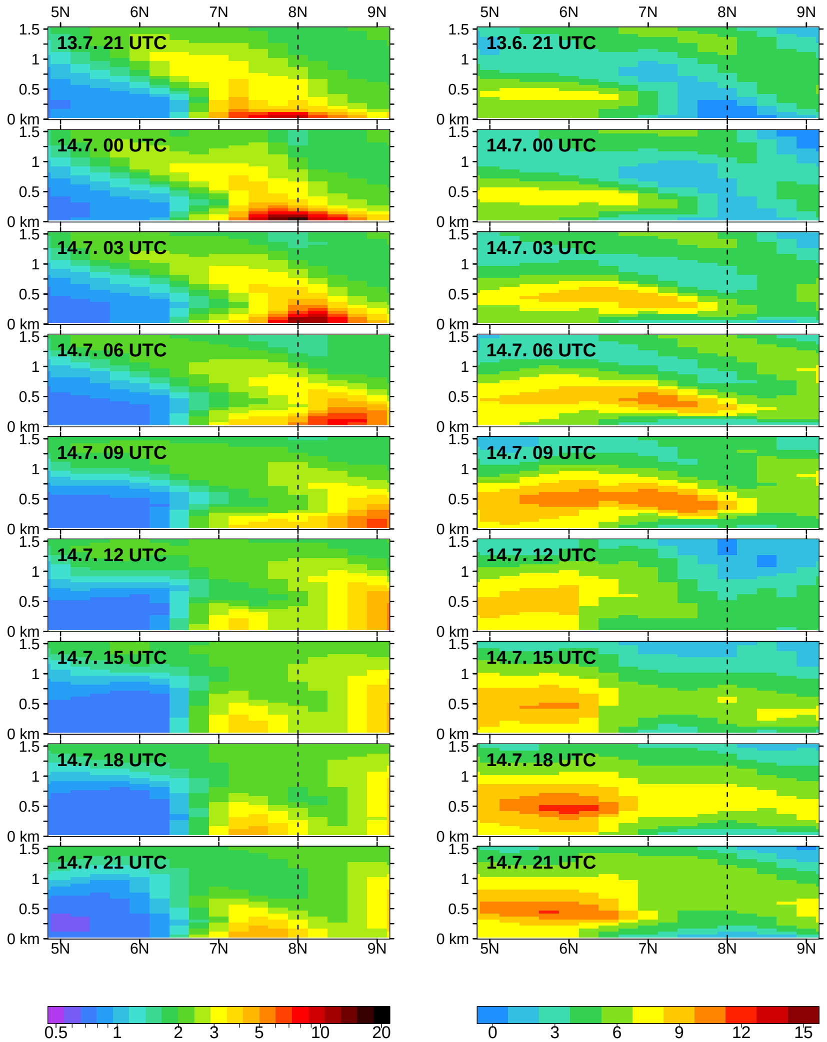

Figure 12. Vertical transect (km a.g.l.) from COSMO-ART of the total BC in $\mu g\,m^{-3}$ (left) and wind speed in $m\,s^{-1}$ (right) along the longitude of Savè between 21:00 UTC on 13 July 2016 until 21:00 UTC on 14 July 2016. The dashed line indicates the location of Savè.

Table 1. Measurements performed with the UAS ALADINA on 14–15 July 2016 during DACCIWA. The table presents the flight time in UTC, cloudy conditions indicated by the lowest cloud base and gas concentrations variations of NO_x and CO during the corresponding flight time as an indicator of local emissions sampled at the Savè supersite by UPS.

Flight number	Day in July 2016	Flight time take off – landing	Cloud base	NO_x	CO
1	14	05:28–06:19 UTC	1200 m	0.7–1.1 ppb_v	158–231 ppb_v
2	14	06:51–07:32 UTC	>2000 m	0.6–0.8 ppb_v	162–195 ppb_v
3	14	11:03–11:43 UTC	1000 m	0.7–1.8 ppb_v	153–203 ppb_v
4	14	12:07–12:56 UTC	800 m	0.6–0.8 ppb_v	146–208 ppb_v
5	14	16:42–17:23 UTC	1000 m	0.9–1.5 ppb_v	179–218 ppb_v
6	14	17:42–18:24 UTC	>2000 m	1.0–1.7 ppb_v	189–232 ppb_v
7	15	05:27–06:13 UTC	1700 m	1.0–1.3 ppb_v	214–249 ppb_v
8	15	06:41–07:24 UTC	300 m	1.4–1.9 ppb_v	224–259 ppb_v
9	15	08:00–08:40 UTC	400 m	1.4–1.9 ppb_v	203–239 ppb_v
10	15	16:48–17:22 UTC	>2000 m	0.8–1.4 ppb_v	156–194 ppb_v
11	15	17:40–18:22 UTC	>2000 m	1.1–1.3 ppb_v	180–215 ppb_v